UNITED NATIONS UNIVERSITY
GEOTHERMAL TRAINING PROGRAMME
Orkustofnun, Grensásvegur 9,
IS-108 Reykjavík, Iceland

Reports 2009
Number 17

# INTERPRETATION OF GEOCHEMICAL WELL TEST DATA FOR WELLS OW-903B, OW-904B AND OW-909 OLKARIA DOMES, KENYA

**Sylvia Joan Malimo**
Kenya Electricity Generating Company Ltd. – KenGen
Olkaria Geothermal Project
P.O Box 785, 20117 Naivasha,
KENYA
*slymalimo@yahoo.com*

## ABSTRACT

Three wells from the Domes field were allowed to discharge for 3 months in early 2009. This report describes the chemical composition of the fluids from these wells, OW-903B, OW-904B and OW-909. Downhole temperatures range from 250 to 350°C which agree with the solute and gas geothermometers. The wells produce fluids with high pH; deep fluid pH ranges from 6.9 to 8.3. OW-909 has higher values for deep fluid TDS, pH and concentrations of anions (B, Cl, F), Na and K than OW-903B and OW-904B. Olkaria Domes wells have a sodium bicarbonate water type similar to those in Olkaria West and Olkaria Central fields. Concentrations of most dissolved constituents were initially low but increased with increasing enthalpy, a considerable range is observed in concentrations. Deep fluids appear to be close to equilibrium with quartz and calcite. Very low Ca concentrations suggest that calcite scaling will not be a problem in the utilization of the Olkaria Domes geothermal fluids.

## 1. INTRODUCTION

The Greater Olkaria geothermal area is situated south of Lake Naivasha on the floor of the southern segment of the Kenya rift (Figure 1). The Kenya rift is part of the East African rift system that runs from Afar triple junction at the Gulf of Eden in the north to Beira, Mozambique in the south. It is the segment of the eastern arm of the rift that extends north from Lake Turkana and south to Lake Natron in northern Tanzania. The rift is part of a continental divergent zone where spreading occurs resulting in the thinning of the crust and the eruption of lavas and associated volcanic activities (Lagat 2004).

The Greater Olkaria geothermal area (GOGA) consists of seven sectors, namely: Olkaria Northeast, Olkaria East, Olkaria Central, Olkaria Southwest, Olkaria Northwest, Olkaria Southeast and Olkaria Domes. This report concentrates on the Olkaria Domes field, which is being developed by the Kenya Electricity Generating Company – KenGen, in addition to two other producing fields, Olkaria East and Olkaria Northeast. This study aims at interpreting the geothermal fluid types, the chemical components and any recommendations resulting thereof in evaluating the chemistry of well discharges from three Olkaria Domes wells (OW-903B, OW-904B and OW-909). The waters of the Domes field are also compared with that in the other six fields in the Greater Olkaria geothermal area.

## 2. BACKGROUND

### 2.1 Location and status of development

Olkaria Domes field is located within the GOGA and lies to the west of Longonot Volcano. Olkaria Domes is the latest of these seven sectors to be deep drilled. Three deep exploration wells were drilled between 1998 and 1999. Approximately 15 wells, both vertical and directional, have been drilled in the Domes area (as of May 2009). Olkaria East and Olkaria Northeast are fully developed with installed capacities of 45 MWe and 70 MWe. Optimization for the two power plants operated by KENGEN in Olkaria East and Olkaria Northeast fields are underway with more wells being drilled in the Olkaria East field. Olkaria Southwest has a 50 MWe binary plant operated by Orpower4 Inc., while a smaller binary plant of ~4 MWe is operated by Oserian Development Company (ODC).

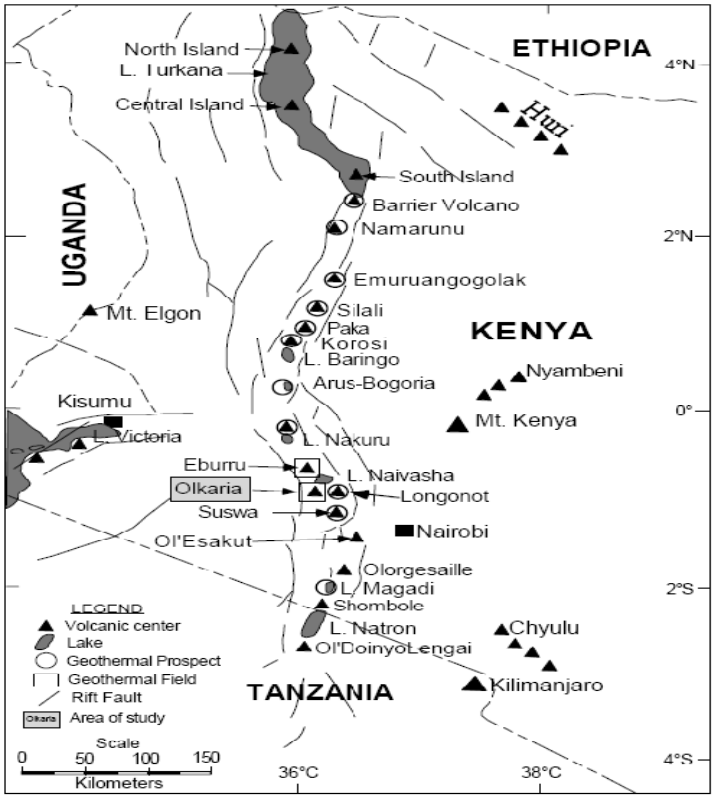


FIGURE 1: Map of the Kenya rift showing the location of Olkaria geothermal field and other quaternary volcanoes along the rift axis (Lagat, 2004)

Olkaria Domes field lies to the east of the Olkaria East field (Figure 2). It is bound approximately by the Hell's Gate National Park, Ol' Njorowa gorge to the west and a ring of domes to the north and south (Mungania, 1999). Most of the Olkaria Domes field lies within the zone defined by the < 20 Ωm apparent resistivity isolines, that covers the central and western portions of the Olkaria Domes prospect. The rest of the field lies within the isoline defining < 30 Ωm apparent resistivity (Onacha, 1993). Three initial exploration wells were sited in the Olkaria Domes field and were drilled to depths varying from 1900 to 2200m vertical depth. These were wells OW-901, OW-902 and OW-903. These wells were sited to investigate the easterly, southerly and westerly extents of the reservoir and the structures that provide fluid flow into

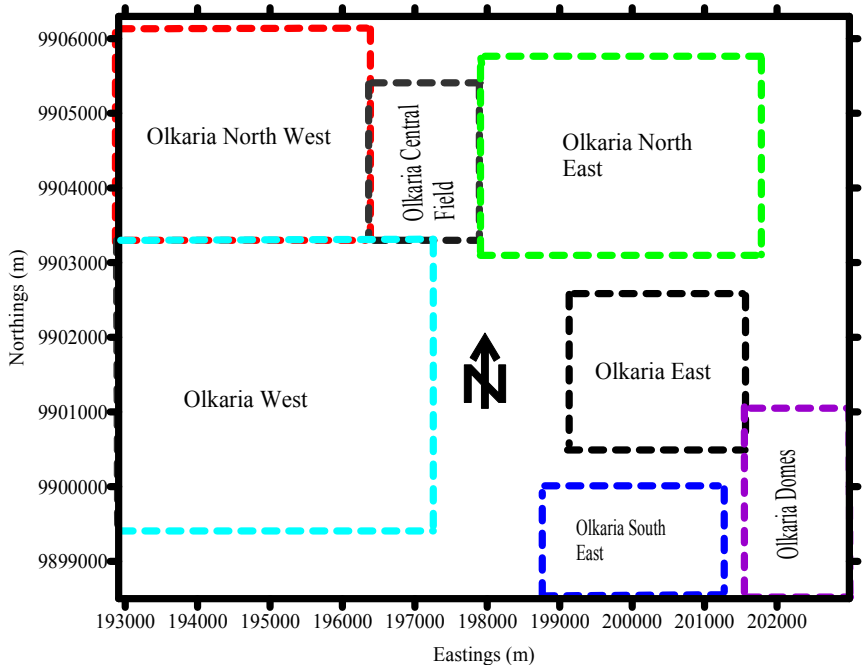


FIGURE 2: Geothermal fields in the Greater Olkaria geothermal area (GOGA) (Opondo, 2007)

the field. Discharge tests were conducted and the fluids characterised. These were of a mixed sodium bicarbonate – chloride – sulphate water type with very dilute chloride concentrations ranging from 178 to 280 ppm (Opondo, 2008).

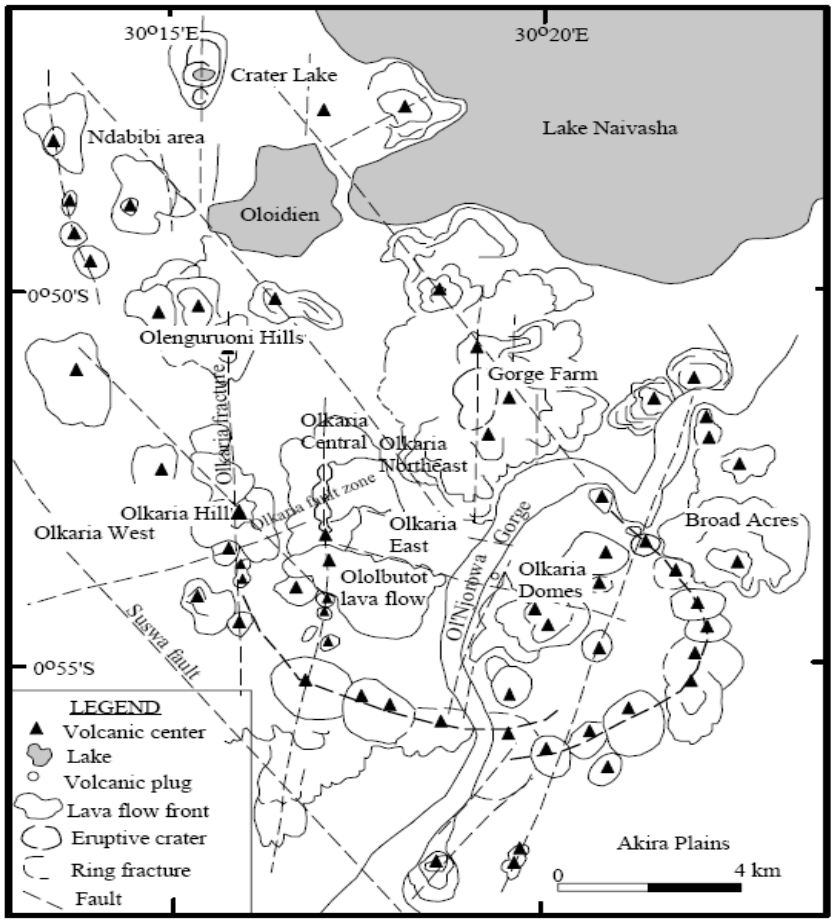


FIGURE 3: Volcano-tectonic map of the Greater Olkaria volcanic complex (modified from Clarke et al., 1990)

## 2.2 Geological setting

The volcanic activity in the Olkaria Domes area has progressed from Miocene to the present with eruption producing rocks ranging from intermediate to acid with minor basic eruptions. Major volcanic and fissure controlled eruptions characterised by caldera collapse phases have resulted in uneven surface topography covered by fresh lava rocks and pyroclastics (Figure 3). Some of the volcanic centres are aligned on an arcuate structure that suggests that the Olkaria complex is a remnant of an older caldera, commonly referred to as the ring structure. The presence of the ring of domes has been used to suggest the presence of a buried caldera (Mungania, 1992). The surface outcrops mainly comprise alkali rhyolite lava flows, pyroclastic deposits, some trachytic and basaltic flows. Pyroclastic deposits comprise compacted and reworked beds and pumice rich deposits which are very thick on the Domes. Some lava dykes up to 6 m thick have been observed to cut across the pyroclastics in a N-S direction. The pyroclastic ash deposits are well layered and vary from weakly to highly weathered often imparting a brownish colour to the deposits (Omenda, 1999).

The Ol'Njorowa gorge is probably an important structural feature that separates the Olkaria East field from the Olkaria Domes field. Comendite is exposed in a few locations along lava fronts and along the Ol'Njorowa gorge. The rocks consist of unconsolidated pyroclastics, alkali rhyolite lavas with intercalations of tuffs, basalts interstratified with trachytes and synetitic intrusives at the bottom of the wells (Mungania, 1999; Omenda, 1999). The eruptive material covering Olkaria volcanic complex area is characterised by acid pyroclastics and alkali rich lavas to an elevation of about 1400 m a.s.l. The high concentrations of incompatible trace elements imply that the volcanic activity tapped the upper parts of a highly fractionated magma reservoir rich in volatiles.

This is further supported by the presence of gas charged magmatic products like pumice and features of explosive volcanism like craters and caldera. According to Clarke et al. (1990), xenoliths of syenite in pyroclastics within the Domes and Longonot areas imply a possible cold or cooling upper part of a magma body which is interpreted to be shallower towards Longonot. The zone between 1400 and 1000 m a.s.l. is dominated by thin basaltic and pyroclastics flows indicating quiet fissure eruptions and

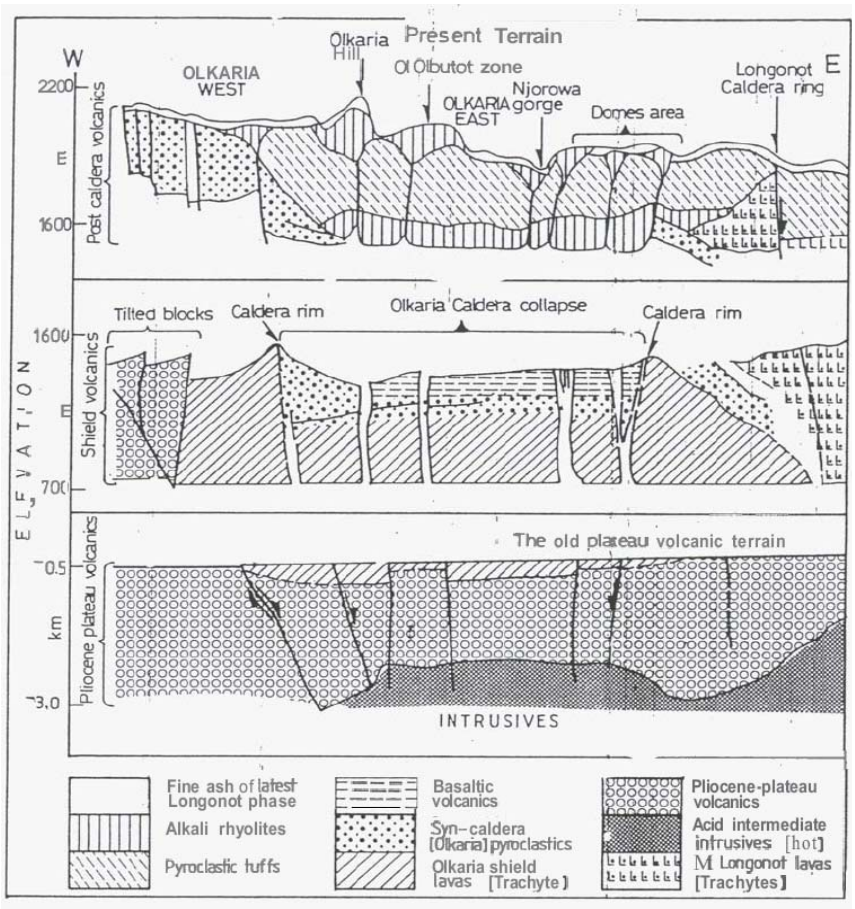


FIGURE 4: Volcanological model of Olkaria Domes area (Onacha and Mungania, 1993)

a period of strombolean type volcanism. Below 1000 m a.s.l., trachytic lava dominates with associated pyroclastics and basalts. The trachytes are further divided into two types. The first is a quartz rich porphyritic type that extends to an elevation of 500 m a.s.l. and may represent remnants of the Olkaria mountain shield lavas. The second is a fine-grained type having a flow texture which may indicate low viscosity associated with Pliocene plateau lavas. Starting from these plateau lavas, the following volcanological model (Figure 4) was put forward (Onacha and Mungania, 1993):

a) The old Pliocene volcanic terrain covered by flood volcanics is characterised by block faulting associated with extensional tectonics.
b) The Plio-Pleistocene shield volcano was built upon the shield quartz-trachyte lavas. The volcano then collapsed and formed a cauldron floor at about 1000-1200 m a.s.l., and due to the emptying of the volatile rich parts of the magma chamber during the explosive caldera collapse phase, more basic magma erupted effusively into the cauldron floor.
c) Reactivation of N-S faults during Pleistocene caused a further explosive withdrawal of magma from a deep differentiated magma chamber. This phase may have been contemporaneous with activity in Longonot.

### 2.3 Previous work

Detailed geological, geophysical and geochemical work was conducted in the area by different researchers (Mungania, 1992). Surface exploration with emphasis on the Olkaria Domes field was conducted in the period 1992-1993 for geophysical, geological and geochemical surveys. This led to the development of a basic working model that resulted in recommendations to drill three wells. Exploration drilling started in June 1998 through June 1999 and three wells were drilled to completion. Three geothermal exploration wells OW-901, OW-902 and OW-903 were drilled in Olkaria Domes field to evaluate its geothermal potential. The three wells (Figure 5) were drilled to a depth of 2200 m and all encountered a high-temperature system and discharged on test. The highest recorded measured temperatures in the wells were: 342°C at -290 m a.s.l., 248°C at 207 m a.s.l. and 341°C at -107 m a.s.l. for wells OW-901, OW-902 and OW-903, respectively. Rocks encountered in the wells include pyroclastics, rhyolite, tuff, trachyte, basalt and minor dolerite and microsyenite intrusives.

Fractures, vesicles, spaces between breccia fragments, glassy rocks and primary minerals exhibit little or no hydrothermal alteration in the upper parts of the wells with mainly silica, calcite, zeolites, phyllosilicates, oxides and sulphides being the alteration minerals present. In the deeper parts of the wells, however, hydrothermal alteration ranges from high to extensive. Hydrothermal zeolites, calcite, epidote, phyllosilicates, silica, sulphides, epidote, albite, adularia, biotite, garnet, fluorite, prehnite, oxides and titanite are the alteration minerals observed. The most important hydrothermal alteration controls in Olkaria Domes field are temperature, rock types and permeability. Figure 6 shows a conceptual geological model of GOGA (Lagat, 2004).

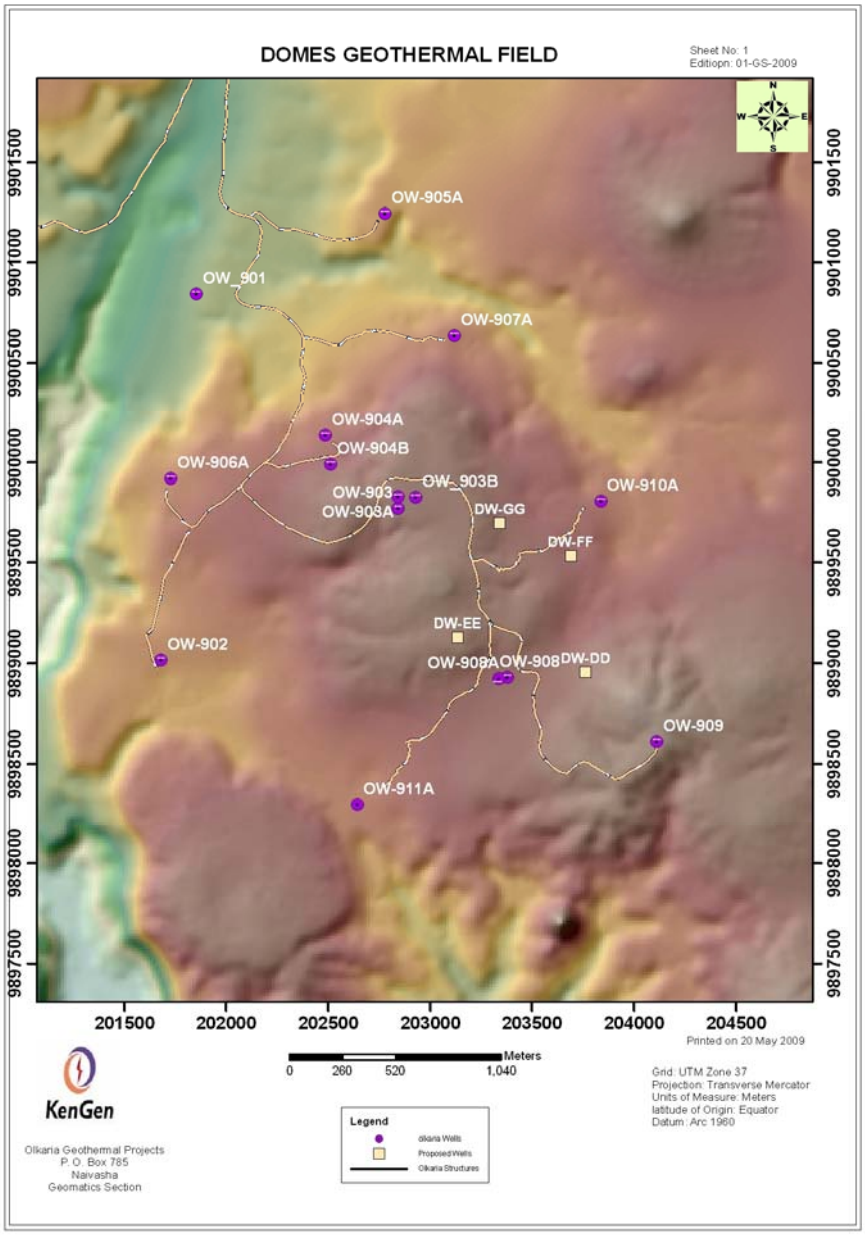


FIGURE 5: Domes map showing the location of wells

Four hydrothermal alteration zones were recognized in the field based on the distribution of the hydrothermal alteration minerals. They are in the order of increasing depth and temperature: the zeolite-chlorite, the illite-chlorite, the illite-chlorite-epidote and the garnet-biotite-actinolite zones. Feeder zones in the wells were found to be confined to faults, fractures, joints and lithologic contacts. Observations from hydrothermal alteration mineralogy, pressure and temperature profiles indicate that well OW-901 is close to the upflow whereas well OW-903 is in the outflow zone and well OW-902 is in the outflow and also the marginal zone of the field. The geochemical analysis found a mixed type sodium bicarbonate-chloride-sulphate water with dilute chloride concentrations (chloride ~178-280 ppm). The pH of fluids discharged tended to be alkali (8.68-10.69) as sampled at atmospheric pressure and analysed at room temperature (25°C). The carbon dioxide gas concentration in steam, on average, was high relative to that of the Olkaria East field. A less mineralised water component was found to exist in this field. Solute geothermometry offered a good estimate of temperatures at dilute fluid inflow into the wells between 1000 and 1200 m. Gas geothermometry approximated the deep temperatures in the reservoir, though these were lower than the measured temperatures at well bottoms (Opondo, 2008).

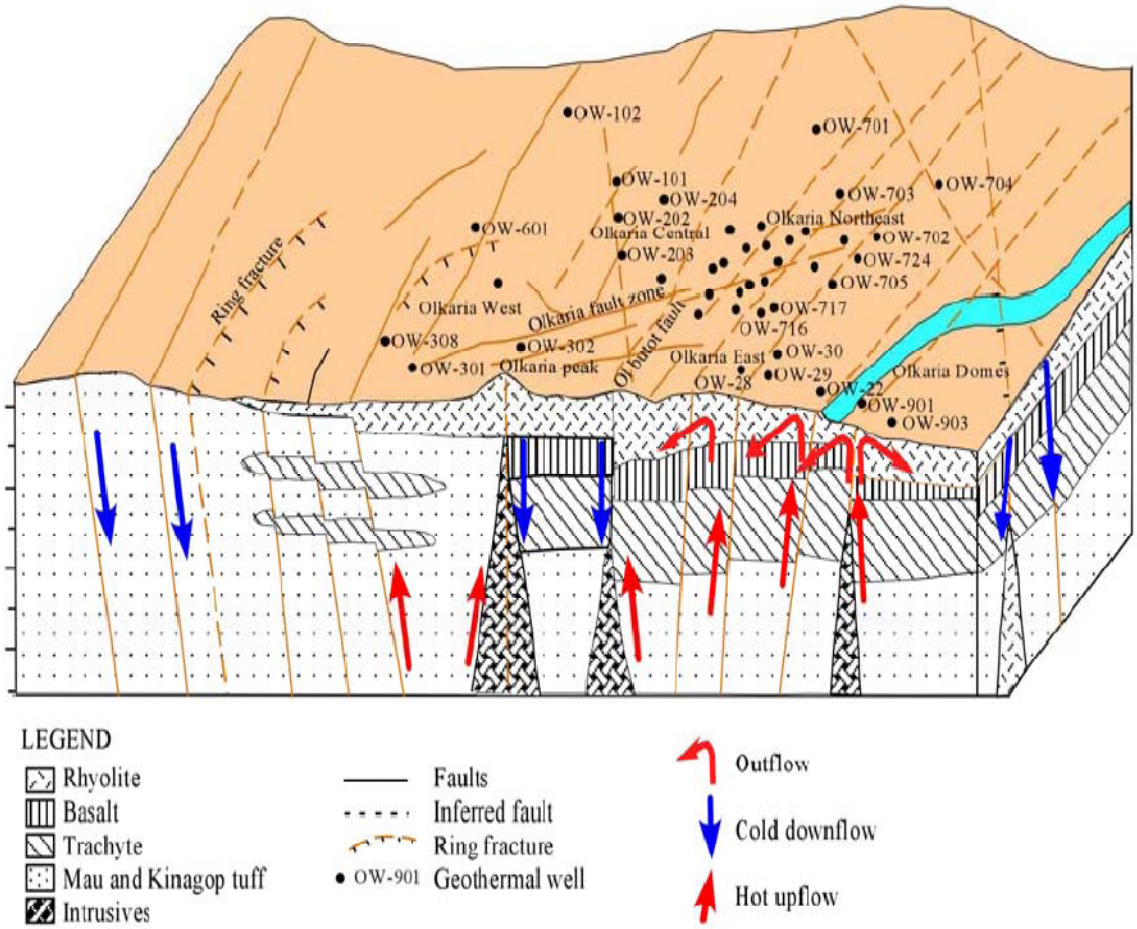


FIGURE 6: A conceptualized geological model of GOGA showing generalized geology and the locations of the fields with respect to downflow, upflow and outflow zones (Lagat, 2004)

### 2.4 Geology of OW-903B, OW-904B and OW-909

The major rock types found during drilling of the three wells selected for this study were trachytes with occurrences of epidotes and basalts. Trachytes dominate from shallow depths with secondary minerals of clays and pyrites. Basalts and tuffs were also observed in the drill cuttings with dominating clay, pyrite and calcite as the secondary minerals.

### 2.5 Reservoir temperature and pressure profiles

The specifications of the three selected wells from the Olkaria Domes are listed in Table 1. Figure 7 shows the temperature logs of the Domes wells for different times during heating, injection and shut in. From these logs, it was possible to select reference temperatures necessary for computing deep fluid compositions from two phase chemical analyses.

TABLE 1: Information on wells OW-903B, OW-904B and OW-909

| Well | Type | Drilled depth (m) | Prod. casing depth (m) | Reference temp. (°C) |
|---|---|---|---|---|
| OW-903B | Directional | 2800 | 1200 | 250 |
| OW-904B | Directional | 2820 | 1200 | 260 |
| OW-909 | Vertical | 3000 | 1200 | 300 |

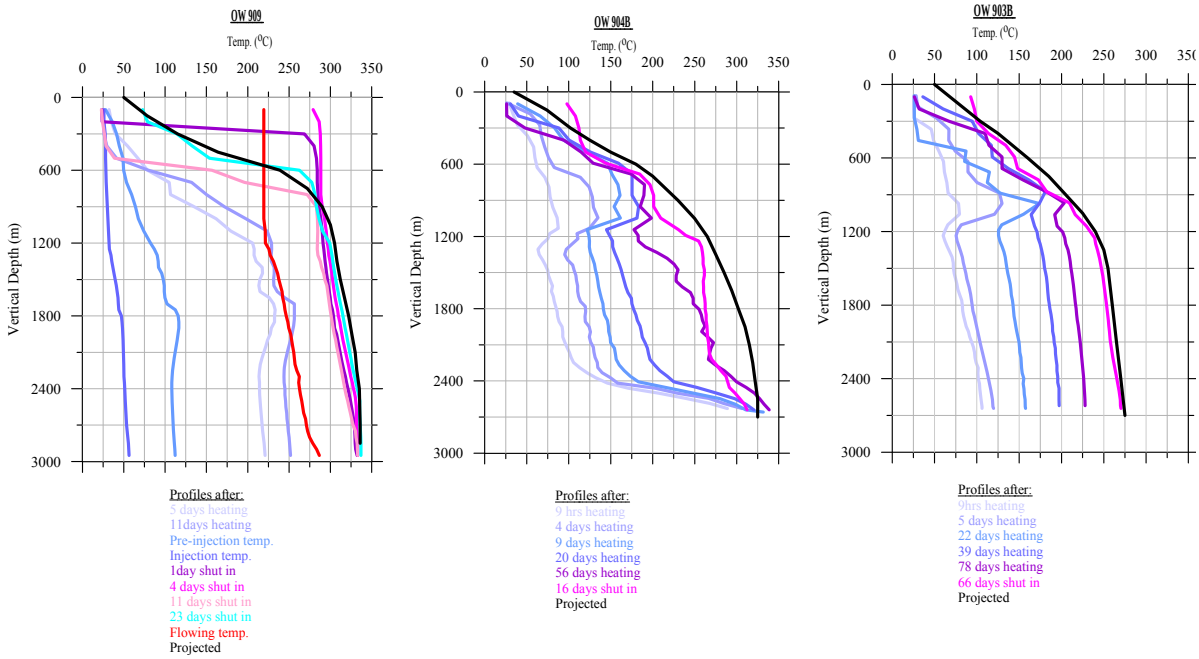


FIGURE 7: Temperature profiles of Olkaria Domes wells

## 3. GEOCHEMICAL DATA AND TRENDS

### 3.1 Sampling and analysis

Water chemistry data is essential information required for the characterization of geothermal fluids and the evaluation of the energy potential of geothermal fields by geothermometry. It also provides good indicators for monitoring reservoir changes in response to production and also allows evaluation and avoiding of scaling problems in wells and surface pipelines. Analytical results with good quality are the key to accurately evaluating geothermal resources and effectively solving reservoir management problems. Collection of samples for chemical analysis is the first step in a long process which eventually yields results that provide information that is used to answer different geochemical questions. In this study two-phase fluid samples from three discharging wells, OW-903B, OW-904B and OW-909 were considered. Steam samples were collected using the Webre separator on the wellhead while the liquid samples were collected at the weir box of the silencer. The liquid samples were collected in plastic bottles while the vapour samples were collected in evacuated double port glass bottles (Giggenbach flasks) containing 50 ml of 40% NaOH. According to Ármannsson and Ólafsson (2006), different ways can be used to preserve the samples. Onsite analysis for $H_2S$ in the water samples, acidification for cations and dilution for silica samples was done. The samples were then analysed for the different elements and gases. Analytical methods for individual components in liquid samples are shown in Table 2. All the gases ($CO_2$, $H_2S$, $CH_4$, $H_2$, and $N_2$) were analysed using gas chromatography.

TABLE 2: Methods used for analysis of different elements in collected samples (Pang and Ármannsson, 2006)

| Analysis | Method |
|---|---|
| pH | pH meter |
| Conductivity / TDS | Conductivity meter / gravimetry |
| $CO_2$ | Titrimetry |
| $H_2S$ | Titrimetry |
| B | Spectrometry |
| $SiO_2$ | Spectrophotometry (with ammonium- molybdate) |
| Na | AAS |
| K | ISE |
| Mg | AAS |
| Ca | AAS |
| F | ISE |
| Cl | Spectrophotometry with thiocyanate |
| $SO_4^{2-}$ | Turbidometry with barium chloride |

### 3.2 Results

The three selected wells in the Domes area of the Olkaria geothermal field were sampled and tested for a period of about 5 months, i.e. from February to June 2009. For data see Appendices I and II. A total of 88 samples were collected. The tables in Appendix I show the raw water and gas data. Most of the samples from the wells had no detectable magnesium and the calcium concentrations were low (less than 10 ppm).

In order to compute the deep fluid composition from the liquid sample (collected at atmospheric pressure) and the steam sample (collected at 1.2-7 bars), it was necessary to recalculate the steam sample composition to atmospheric pressure. The atmospheric steam composition was combined with the liquid sample composition in the computation of the deep fluid composition using the WATCH program Version 2.1 (Arnórsson and Bjarnason, 1994). Samples with good ionic charge balance (charge balance from -10 to +10) were then speciated using the WATCH program to give concentrations of the deep fluids (Appendix II). For any solution, the total charge of positively charged ions will equal the total charge of negatively charged ions in reality as the net charge for any solution must equal zero. In the samples analyzed, though, the charge balances were not equal to zero, hence the samples with the closest charge balance, i.e. ±10, were used.

## 4. GEOCHEMICAL DATA INTERPRETATION

### 4.1 Trends with time in the composition of well discharges

A total of 88 samples were used to compute the trends of the three wells sampled during discharge. The different solute and gas components were monitored and sampled to evaluate the recovery of the wells after shut in. Appendix II shows the trends in the different components monitored for a period of about 100 days. OW-909 seems to have higher concentrations of the cation components as compared to OW-903B and OW-904B. Despite the limited time of recovery, the sulphate concentrations declined with time as the $H_2S$ concentrations increased showing good geothermal water inflow into the wells. The scatter in the data might in part result from non-equilibration of the geothermal water and the drilling fluids that had not been totally discharged from the wells and to some degree it might reflect analytical uncertainties.

### 4.2 Correlation of discharge components with chloride

Plots depicting the concentrations of several components such as B, $SiO_2$, Ca, Na, K and F as a function of Cl concentration are shown in Appendix III. These plots seem to indicate that the ratios of chloride are close to being linear with regards to the other components except with calcium which is in very low concentrations in these new wells. The concentrations of dissolved constituents in the fluids from wells OW-904B and OW-903B tend to be very similar whereas the fluids from well OW-909 tended to have higher concentrations of dissolved solids.

### 4.3 Cl-$SO_4$-$HCO_3$ ternary diagram

According to Giggenbach (1991), ternary diagrams are used for the classification of thermal water based on the relative concentrations of the three major anions $Cl^-$, $SO_4^{2-}$ and $HCO_3^-$. Chloride, which is a conservative ion in geothermal fluids, does not take part in reactions with rocks after it has dissolved. Chloride does not precipitate after it has dissolved; its concentration is independent of the mineral equilibria that control the concentrations of the rock-forming constituents. Thus, chloride is used as a tracer in geothermal investigations. The Cl-$SO_4$-$HCO_3$ ternary diagram is one diagram for classifying natural waters (Giggenbach, 1991). Using it, several types of thermal water can be distinguished: mature waters, peripheral waters, steam-heated waters and volcanic waters. The diagram provides an initial indication of mixing relationships. According to Giggenbach (1991), the chloride-rich waters are generally found near the upflow zones of geothermal systems. High $SO_4^{2-}$ steam-heated waters are usually encountered over the more elevated parts of a field. The degree of separation between data points for high chloride and bicarbonate waters may give an idea of the relative degree of interaction of the $CO_2$ charged fluid at lower temperature, and of the $HCO_3^-$ concentrations which increases with time and distance travelled underground.

Figure 8 shows that the three Olkaria Domes wells (OW-903B, OW-904B and OW-909) plot in the region of high $HCO_3$ peripheral waters and low chloride. This illustrates that the geothermal fluids in the Olkaria Domes reservoir are bicarbonate waters and correspond to peripheral waters (Giggenbach, 1991). The figure also shows the correlation of the waters with those of the other fields in the GOGA. The Olkaria Domes fluids seem to plot similar to those of Olkaria West and Olkaria Central fields. From the relative abundance of chloride, sulphate and bicarbonate of the Olkaria wells, these waters would be classified as sodium-chloride and sodium-bicarbonate water, or mixtures thereof (Figure 8). Wells in the Olkaria East production field and in Olkaria Northeast discharge sodium-chloride type water, classified as more mature according to the scheme of Giggenbach (1991).

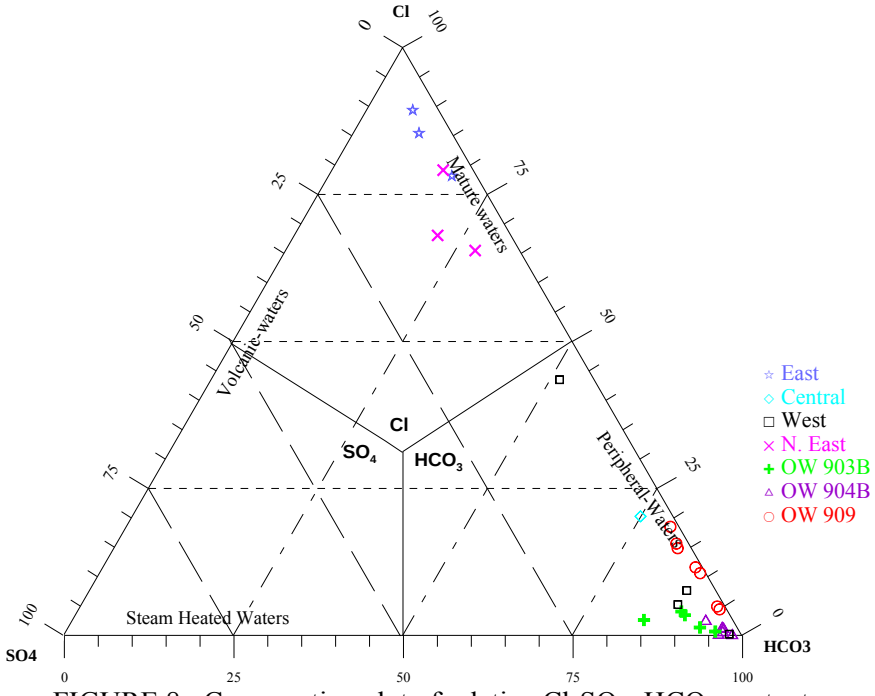


FIGURE 8: Comparative plot of relative Cl-$SO_4$ -$HCO_3$ contents from the discharges of wells in the GOGA fields

### 4.4 Relative Cl, Li and B contents

Lithium is used as a tracer, because it is the alkali metal least affected by secondary processes for initial deep rock dissolution, and as a reference for evaluating the possible origin of two important 'conservative' constituents of geothermal waters, Cl and B. Once added, Li largely remains in the solution. The B content of thermal fluids is to some degree likely to reflect the maturity of a geothermal system; because of its volatility it is expelled during the early heating up stages. In such a case, fluids from older hydrothermal systems can be expected to be depleted in B while the inverse holds for younger hydrothermal systems. It is, however, striking that both Cl and B are added to the Li containing solutions in proportions close to those in crustal rocks. At higher temperatures, Cl occurs as HCl and B as $H_3BO_3$. Both are volatile and can be mobilized by high-temperature steam. They are, therefore, quite likely to have been introduced with the magmatic vapour invoked above to lead to the formation of deep acid brine responsible for rock dissolution (Karingithi, 2000).

At low temperatures the acidity of HCl increases rapidly, and is soon converted by the rock to the less volatile NaCl. B remains in volatile form to be carried in the vapour phase even at lower temperatures. The Cl/B ratio is often used to indicate a common reservoir source for the waters. Care must, however, be taken in applying such an interpretation since waters from the same reservoir may show differences in this ratio, due to changes in lithology at depth over a field (example, the occurrence of a sedimentary horizon), or by the absorption of B into clays during lateral flow.

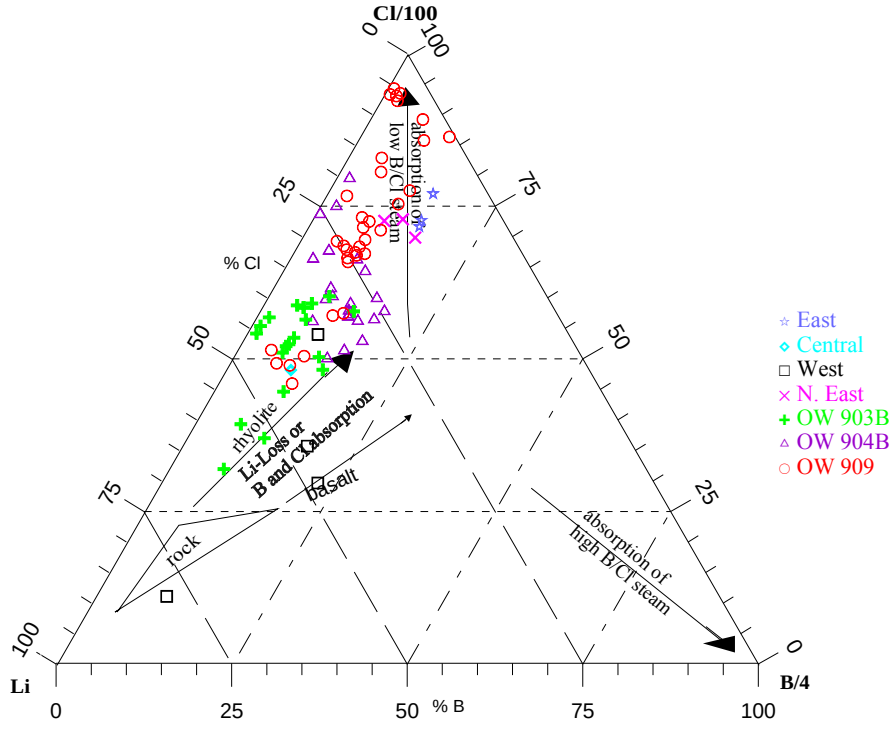


FIGURE 9: Comparative plot of relative Cl, Li, and B from discharges of wells in the GOGA fields

The fluids from the Olkaria Domes wells OW-903B, OW-904B and OW-909 plot (Figure 9) in the region along the Li-Cl axis but do not cluster around the same point. B/Cl ratios are in the intermediate region and could suggest the absorption of low B/Cl magmatic vapours. Discharges from the Olkaria-Domes wells show comparatively low lithium content. This is also shown in fluids from the other GOGA wells.

### 4.5 Geothermometry

Chemical geothermometers are based on the assumption that temperature dependent mineral solute equilibrium is attained in the geothermal reservoir. In this report, chemical geothermometers were used to assess the reservoir temperatures for the three wells chosen from Olkaria Domes. Studies indicate that geothermal water compositions are controlled by a close approach to mineral-solution equilibria with respect to various elements (Arnórsson et al., 1983a; Tole et al., 1993; Karingithi, 2000). Changes, which occur in temperature and water composition during boiling between aquifer

and wellhead, generally lead to changes in mineral saturation. Such changes may result in mineral precipitation or mineral dissolution. Chemical geothermometry is based on constituents that are resistive to such secondary changes.

### 4.6 Solute geothermometers

In geochemical studies, water chemistry and gas composition of geothermal fluids have proven useful in assessing the characteristics of geothermal reservoirs, both to estimate temperatures (Arnórsson and Gunnlaugsson, 1983; D'Amore and Truesdell, 1985) and to estimate initial steam fractions in the reservoir fluid (D'Amore and Celati, 1983; D'Amore and Truesdell, 1985). The following solute geothermometers were used in this study:

| | | | |
|---|---|---|---|
| *Quartz* | Fournier (1977) | *Na-K* | Arnórsson et al. (1983) |
| | Fournier and Potter (1982) | | Giggenbach (1988) |
| | Fournier (1979) | | |

#### 4.6.1 Silica geothermometers

The silica geothermometers are based on experimentally determined solubilities of chalcedony and quartz. Usually the quartz geothermometer is applied to high-temperature reservoirs like the Olkaria geothermal field. Application of the silica geothermometers is based on the fact that the activity of dissolved silicic acid, $H_4SiO_4$, in equilibrium with quartz, is temperature dependent. The solubility reactions for silica minerals can be expressed as:

$$SiO_{2,solid} + 2H_2O = H_4SiO_4{}^o \quad (1)$$

However, $H_4SiO_4{}^0$ is not only aqueous silica species in natural waters. $H_4SiO_4{}^0$ is a weak acid which dissociates if the pH of the fluid is high enough to yield $H_3SiO_4{}^-$:

$$H_4SiO_4{}^0 = H^+ + H_3SiO_4{}^- \quad (2)$$

Analysis of silica in aqueous solution yields the total silica concentration, generally expressed as ppm $SiO_2$, which includes both un-ionized $H_4SiO_4{}^0$ and ionized ($H_3SiO_4{}^-$). The dissociation constant for silicic acid is about $10^{-10}$ at 25°C. Thus, at a pH of 10 ($H^+ = 10^{-10}$), the concentration of unionized silica equals that of ionized silica (note chemical formula in brackets refers to the activity of the indicated species for mineral):

$$K_{H_4SiO_4{}^\circ} = \frac{[H^+][H_3SiO_4{}^-]}{[H_4SiO_4{}^\circ]} \quad (3)$$

When using quartz geothermometers, some factors should be considered (Fournier and Potter, 1982):

- The temperature range in which the equations are valid;
- Possible polymerization or precipitation of silica before sample collection;
- Possible polymerization of silica after sample collection;
- Control of aqueous silica by solids other than quartz;
- The effect of pH upon quartz solubility; and
- Possible dilution of hot water with cold water before the thermal waters reach the surface.

The quartz geothermometers used to estimate the aquifer temperatures in this report are:

*Fournier (1977):*

$$t\ (°C) = \frac{1309}{5.19 - logS} - 273.15 \quad (4)$$

*Fournier and Potter (1982):*

$$t(°C) = -42.2 + 0.28831S - 3.6686 \times 10^{-4}S^2 + 3.1665 \times 10^{-7}S^3 + 77.034 \log S \quad (5)$$

The results for the quartz calculations are shown in Table 3.

### 4.6.2 Cation geothermometers

Reactions between alkali feldspars and Na and K in aqueous solution have often been described as exchange reactions. At the temperature prevailing in geothermal systems, the reaction involves simultaneous equilibrium between $Na^+$ and $K^+$ in solution and quite pure albite and K-feldspar. The reaction is expressed as:

$$NaAlSi_3O_8 + K^+ = KAlSi_3O_8 + Na^+ \quad (6)$$

The equilibrium constant, $K_{eq,}$ for Reaction 6 is:

$$K_{eq} = \frac{[KAlSi_3O_8][Na^+]}{[NaAlSi_3O_8][K^+]} \quad (7)$$

The activities of the solid reactants are assumed to be in unity and the activities of the dissolved species are taken to equal to their molal concentrations in aqueous solution. Equation 7 reduces to:

$$K_{eq} = \frac{[Na^+]}{[K^+]} \quad (8)$$

In this report, the following equations were used for calculating reservoir temperatures based on the Na/K activity ratio in the geothermal fluid:

*Fournier (1979):*

$$t(℃) = \frac{1217}{1.438 + \log(Na/K)} - 273.15 \quad (9)$$

*Arnórsson et al. (1983)* – temperature range 250-350°C:

$$t(℃) = \frac{1319}{1.699 + \log(Na/K)} - 273.15 \quad (10)$$

*Giggenbach (1988):*

$$t(℃) = \frac{1390}{1.750 + \log(Na/K)} - 273.15 \quad (11)$$

The reference temperatures chosen agree with the different chosen geothermometers. OW-903B has aquifer temperatures in the range of 220-260°C; OW-904B has temperatures in the range of 230-300°C while OW-909 temperatures are in the range of 250-340°C, indicating good production temperatures. The results for the calculations are shown in Table 3.

### 4.7 Gas geothermometers

Studies in many high-temperature geothermal fields (> 200°C) indicate that the concentrations (or ratios) of gases like $CO_2$, $H_2S$, $H_2$, $N_2$, $NH_3$, and $CH_4$ are controlled by temperature-dependent gas-gas and/or mineral-gas equilibria (D'Amore and Arnórsson, 2000). On this basis, data from chemical analyses of those gases have been used to develop relationships between the relative gas concentrations and the temperature of the reservoir. Such relationships are known as *gas or steam geothermometers*. Gas geothermometers are also based on certain chemical reactions between gaseous species and minerals which are considered to be in chemical equilibrium. For each chemical equilibrium considered, a thermodynamic equilibrium constant may be expressed in terms of temperature, in which case the concentration of each gas species is often represented by its partial pressure in the vapour phase (D'Amore and Truesdell, 1985).

Geothermal gases are introduced into geothermal fluid with recharge water, from water-rock interaction in the reservoir or from magmatic fluid invasion. In an undisturbed reservoir, reactions in equilibrium at the reservoir temperature control the concentrations of these gases. Upon boiling, the partitioning of gases between the liquid and vapour phase is controlled by the enthalpy of the geothermal fluid and the boiling temperature in cases where the vapour travels without hindrance to the surface (in boreholes and wide open fissures), then negligible changes in the gas concentrations and ratios will occur, and these can be used as gas geothermometers. There are essentially three types of gas geothermometers. The first group is based on gas-gas equilibria. The second group is based on mineral-gas equilibria involving $H_2S$, $H_2$ and $CH_4$ but assuming $CO_2$ to be externally fixed. The third group is based on mineral-gas equilibria. The first two groups of geothermometers require only data on the relative abundance of gaseous components in the gas phase, whereas the third group calls for information on gas concentrations in steam (D'Amore and Arnórsson, 2000).

When using gas geothermometry, it is important to keep in mind that several factors other than aquifer temperature may affect the gas composition of a geothermal fluid. In geothermal reservoir fluids, gas concentrations at equilibrium depend on the ratio of steam to water of that fluid, whereas the gas content of fumarole steam is also affected by the boiling mechanism in the upflow, steam condensation and the separation pressure of the steam from the parent water. Furthermore, the flux of gaseous components into geothermal systems from their magmatic heat source may be quite significant and influence how closely gas-gas and mineral-gas equilibria are approached in specific aquifers (D'Amore and Arnórsson, 2000). In this study, the gas geothermometers used are those based on gas concentrations in mmol/kg corrected to the atmospheric pressure. The geothermometers are based on mineral gas equilibria and the temperature equations for the thermodynamic data for the following reactions:

$$2Ca_2Al_3Si_3O_{12}(OH) + 2CaCO_3 + 3SiO_2 + 2H_2O = 3Ca_2Al_2Si_3O_{10}(OH)_2 + 2CO_{2,aq} \quad (12)$$

$$FeS_2 + FeS + 2Ca_2Al_2Si_3O_{10}(OH)_2 + 2H_2O = 2Ca_2Al_2FeSi_3O_{12}(OH) + 3H_2S_{aq} \quad (13)$$

$$4FeS + 2Ca_2Al_2Si_3O_{10}(OH)_2 + 2H_2O = 2Ca_2Al_2FeSi_3O_{12}(OH) + 2FeS_2 + 3H_{2,aq} \quad (14)$$

Q in the gas geothermometry equations represents the gas concentrations in log mmol/kg. The geothermometer equations are (Arnórsson, 1998):

*$T_{CO_2}$:*

$$\mathrm{t(°C)} = 4.724\mathrm{Q}^3 - 11.068\mathrm{Q}^2 + 72.012\mathrm{Q} + 121.8 \quad (15)$$

*$T_{H_2}$:*

$$t(°\mathrm{C}) = 6.630Q^3 + 5.836Q^2 + 56.168Q + 227.1 \quad (16)$$

$T_{CO_2/N_2}$:

$$t(°C) = 1.739Q^3 + 7.599Q^2 + 48.751Q + 173.2 \quad (17)$$

The results in Table 3 show the different geothermometer results found for the three wells. The samples used to calculate for the geothermometers are those that had all the elemental analyses; the samples used to calculate the geothermometers had been discharged for a while to give a good indication of the reservoir fluid and good charge balances per well were also considered.

TABLE 3: Various solute and gas geothermometers of Olkaria Domes wells

| Well | $T_{q-1}$ | $T_{q-2}$ | $T_{NaK-1}$ | $T_{NaK-2}$ | $T_{NaK-3}$ | $T_{qtz}$ | $T_{NaK}$ | $T_{CO2}$ | $T_{H2}$ | $T_{CO2/N2}$ | $T_{ref.}$ | $T_{av.}$ | $T_{median}$ |
|---|---|---|---|---|---|---|---|---|---|---|---|---|---|
| OW-903B | 232 | 238 | 263 | 248 | 265 | 249 | 245 | 221 | 239 | 259 | 250 | 246 | 248 |
| OW-904B | 254 | 266 | 271 | 255 | 272 | 276 | 307 | 244 | 228 | 263 | 260 | 263 | 263 |
| OW-909 | 274 | 294 | 339 | 351 | 332 | 264 | 340 | 253 | 300 | 268 | 300 | 301 | 300 |

$T_{q-1}$ Fournier, 1977 $T_{q-2}$ Fournier and Potter, 1982
$T_{NaK-1}$ Fournier, 1979 $T_{NaK-2}$ Arnórsson et al., 1983
$T_{NaK-3}$ Giggenbach, 1988 $T_{qtz}$ WATCH calculated quartz
$T_{NaK}$ WATCH calculated Na-K $T_{ref}$ Observed temperatures
$T_{av.}$ Average temperature $T_{median}$ Median temperature
$T_{CO_2}$, $T_{H_2}$, $T_{CO_2/N_2}$ Arnórsson, 1998

### 4.8 Deep fluid species, log Q/K and saturation indices

As previously stated in the geothermometry section above, the WATCH programme was used to speciate for the deep fluids. Quartz in the deep fluids shows a slight undersaturation with a bit of scatter due to non-equilibration of the deep fluids and the drilling fluids during the discharge testing (Figure 10). The initial discharge samples were quite varied as compared to the later sampled ones which show equilibration with the quartz species. For the calcite deep fluid species, both the WATCH and SOLVEQ programmes were used to speciate the samples. The SOLVEQ program was used to compute for the calcite because WATCH results always predicted super saturation that was not a realistic result for nature. With SOLVEQ, we get a more realistic result because it incorporates more Ca bearing species like $CaCl^+$, $CaCl_{2\ (aq)}$, $CaF^+$ and $Ca(HSiO_3)^+$ apart from the ones that both programs incorporate ($Ca_2^+$, $CaSO_{4(aq)}$, $CaHCO_3^+{}_{(aq)}$ and $CaOH^+$).

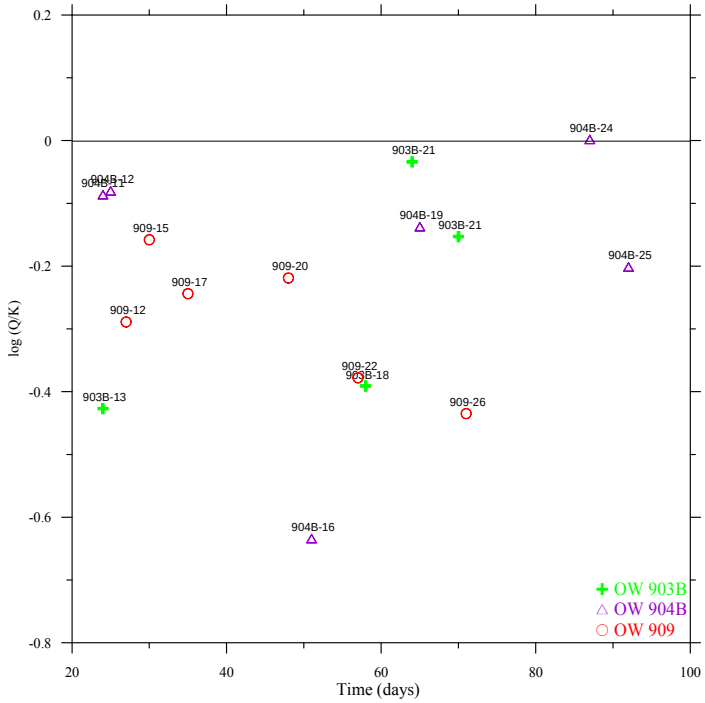


FIGURE 10: Quartz saturation of the deep fluids from Olkaria Domes field

Using the results of the aqueous speciation calculations, the saturation indices (SI) of minerals in aqueous solutions at different temperatures were computed. The SI value for each mineral is a measure of the saturation state of the water phase with respect to the mineral phase. Values of SI greater than, equal to, and less than zero represent super saturation, equilibrium and under-saturation, respectively, for the mineral phase with respect to the aqueous solution. Equilibrium constants for mineral dissolution often vary strongly with temperature. Calcite

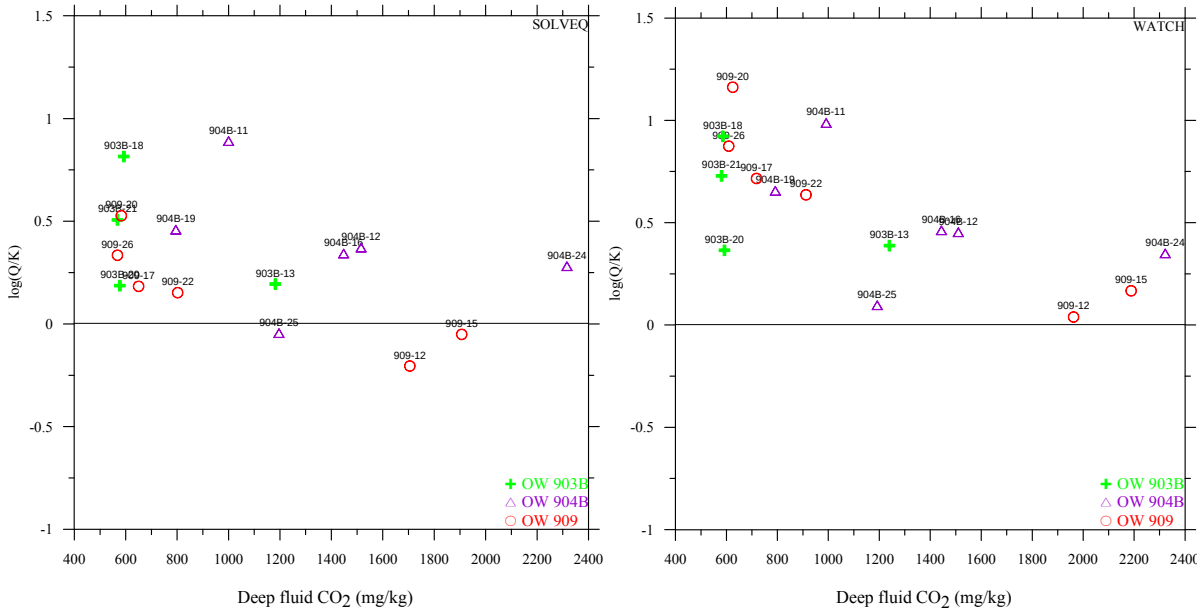


FIGURE 11: Calcite saturation of deep fluids from Olkaria Domes wells

seems to be close to the super saturation line with few exceptions (Figure 11). In these samples, although low calcium concentrations were detected, the concentration was expected to equilibrate with time as the well flows and the chemical composition of the deep fluids reach equilibrium.

## 5. PRODUCTION PROPERTIES

Brine handling can be difficult in geothermal operations. It is frequently described as the entire periodic table of elements in a pipe. The high-temperature solution of elements and compounds, however, causes operational limitations in geothermal power plants. These limitations are due to the severe scaling and corrosion characteristics of geothermal brine and steam. Because of these characteristics, plants may experience extreme plugging and corrosion in wells, lines and equipment. Curtailment in power plant production and even complete plant shutdown are often the end results from these conditions. Different types of brine with differing chemistry conditions are found in various areas around the world. Substantial differences can even be found within the various wells of a given field, as seen in the new Olkaria Domes field. The chemistry of these different brines varies and the differences depend on several factors including the geology of the resource, temperature, pressure, and water source. Depending on the resource, steam and water ratios in the brine can vary significantly.

The scaling characteristics of brine and steam cause difficult problems in geothermal operation. The variety of problems associated with handling geothermal brine can be extreme – making it critical to understand the chemistry of the brine for successful plant operation. Geothermal brine causes a variety of operational problems and includes the following:

- Equipment damage and failure;
- Equipment repair and replacement;
- Well and line plugging;
- Reduced steam/brine flow;
- Power production losses; and
- Complete or partial plant shutdown.

The effectiveness of the development of geothermal energy will be determined by the amount of geothermal power that is made available, and this amount will be influenced by the effect that material problems have on efficiency and downtime. Since every technological effort is limited to some extent by the performance of materials, it is prudent to consider scaling and corrosion and material problems which may limit the development of geothermal energy. The availability of durable and cost-effective construction materials for processing geothermal fluids has a definite impact on the development of geothermal energy. Geothermal resources include steam-dominated sources, liquid dominated sources, geo-pressurized sources, and dry (hot rock) sources. Scale is a major problem in geothermal operation. The plugging and deposit problems caused by scaling can reduce power plant production, and create expensive cleaning costs. The reduction in power and increased operating costs caused from difficult scale conditions can directly impact a plant's financial outcome. Different types of scales are found in various geothermal areas and, sometimes, even within the various wells of the same field. The major species of scale in geothermal brine typically include calcium, silica and sulphide compounds (Stapleton, 2002).

To be able find the production properties of the three Olkaria Domes wells, three samples were used to analyse the deep fluid calcite and silica saturation. The species selected for this speciation were those sampled later in the discharge testing period so as to get as close as possible to equilibrium fluids and thus the silica and calcite concentrations. The samples selected for silica analysis also had good charge balance and the highest silica concentrations to find the speciation for the deep fluid silica concentration. The samples selected for calcite scaling evaluation had the lowest calcium concentration but representative pH values and $CO_2$ concentration.

## 5.1 Scaling

Geothermal waters are saturated with silica and are frequently close to saturation with calcite, calcium sulphate and calcium fluoride. Some acid hot water also contains appreciable concentrations of heavy metals. Changes in temperature and pressure disturb the equilibria and will generally lead to scale formation. Calcite and silica deposits are the most frequent scale formation materials. The most troublesome calcite deposits usually occur in the well casing at the level of first boiling (bubble point) with heavy bands of calcite depositing over a short length (Moller et al., 2004).

### 5.1.1 Silica scaling

Silica related scale is arguably one of the most difficult scales occurring in geothermal operation. Silica is found in virtually all geothermal brine and its concentration is directly proportional to the temperature of the brine. As brine flows through the well to the surface, the temperature of the brine decreases, silica solubility decreases correspondingly and the brine phase becomes over saturated. When pressure drops in the flash vessel, steam flashes and the temperature of the brine further decreases. In the flash vessel, the brine phase becomes more concentrated. Under these conditions, silica precipitates as either amorphous silica or it will react with available cations (e.g. Fe, Mg, Ca, Zn) and form co-precipitated silica deposits.

Scale formation in plant equipment and porosity losses in injection well formations created by the precipitation of amorphous silica have been identified as important problems in some geothermal power operations. In high-temperature hydrothermal systems, the formation water is frequently in near equilibrium with quartz. Since the solubilities of pure silica minerals decrease rapidly with decreasing temperature, large amounts of quartz would be expected to precipitate as the brines in these systems are cooled upon production and energy extraction. However, quartz rarely precipitates because of the slow kinetics involved in this reaction. Although amorphous silica has a higher solubility than quartz, it is a much more common precipitate in geothermal operations (Moller et al., 2004). The solubility reactions for silica minerals are invariably expressed in Equations 1 and 2.

Since geothermal waters may boil in the upflow of the geothermal system if reservoir temperatures are above 100°C, the boiling causes the concentrations of aqueous solutes to increase in proportion to the steam fraction. It also causes the pH of the water to increase because the weak acids dissolved in the water, $CO_2$ and $H_2S$, are transferred into the steam phase. To estimate the silica scaling in the new wells drilled in the Olkaria Domes field, the WATCH program was used to speciate the analysis and the results indicated on the graphs. From Equations 2 and 3, it can be seen that $H_4SiO_4^0$ is not the only aqueous silica species in natural waters. $H_4SiO_4^0$ is a weak acid which dissociates, if pH of the fluid is high enough to yield $H_3SiO_4^-$. Boiling the fluids, thus, affects the silica concentration, causing the activity of silica to decrease and finally precipitate as amorphous silica at the temperatures shown in Figure 12.

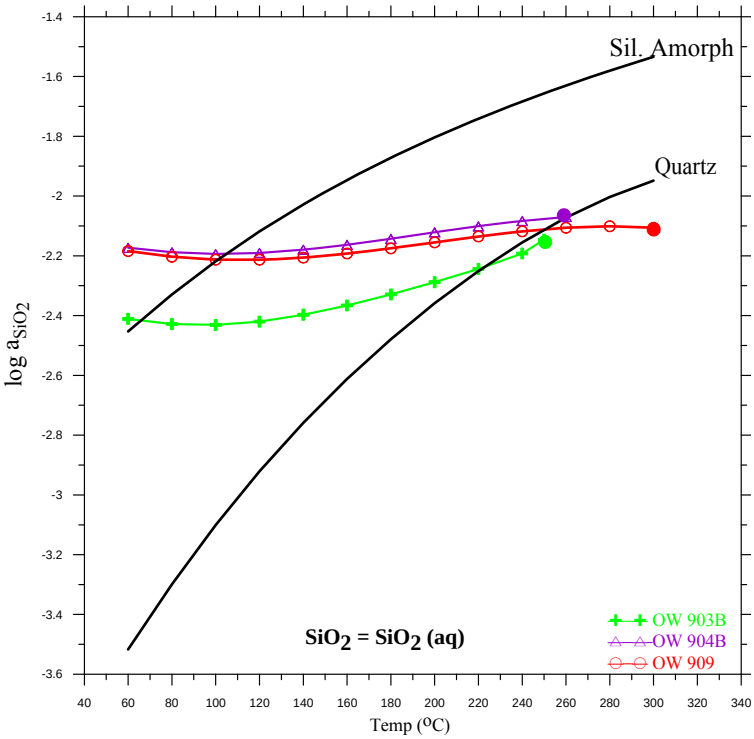


FIGURE 12: Quartz saturation during boiling of fluids from Olkaria Domes field

### 5.1.2 Calcite scaling

Calcite, a major scale-forming mineral in many geothermal systems, precipitates from a brine according to the following reaction:

$$Ca^{2+}(aq) + 2HCO^-_3 \leftrightarrow CaCO_3(s)\downarrow + H_2O + CO_2\uparrow \quad (18)$$

Ocampo-Diaz et al. (2005) found that scale deposition, especially calcite ($CaCO_3$), is a complex function of physical chemistry (for example, total salinity, pH and concentration of calcium and dissolved $CO_2$) and the pH change upon boiling compared to the rate of cooling upon boiling. Calcite is commonly saturated in the reservoir fluid, and when such fluids boil there is generally a chemical potential to form calcite. However, unlike silica and the sulphides, calcite becomes more soluble as temperature decreases. As a result, the most severe calcite scale deposition tends to occur for lower temperature geothermal fluids, below 220-240°C.

When Reaction 18 is forced to the right by the loss of $CO_2$ from the liquid phase into a gas phase on flashing, calcite is deposited. In complex brines there may be many other reactions taking place, some of which interact with the calcium and carbonate ions. For this prediction, a sample from each well was selected. The samples selected (20, 25 and 22 for wells OW-903B, OW-904B and OW-909, respectively) had a representative pH and $CO_2$ with reference to the others from the wells. Although the general calcium concentration was low for these wells, the $CO_2$ and pH were considered for sample selection. The results from the wells during the initial discharge seemed to have low concentrations of calcium (and high pH values) but trends indicate that with further discharge, the calcium concentrations would increase though not to a great extent. From the WATCH calculations, the calcite saturation was over estimated, but considering the deep fluids shown (Figure 11) were at equilibrium with calcite when the boiling started, then less super saturation would have been

experienced during boiling. Calcite scaling will not be a problem in these Domes wells (Figure 13) as indicated by the low calcium concentrations and high pH (which affects calcite saturation).

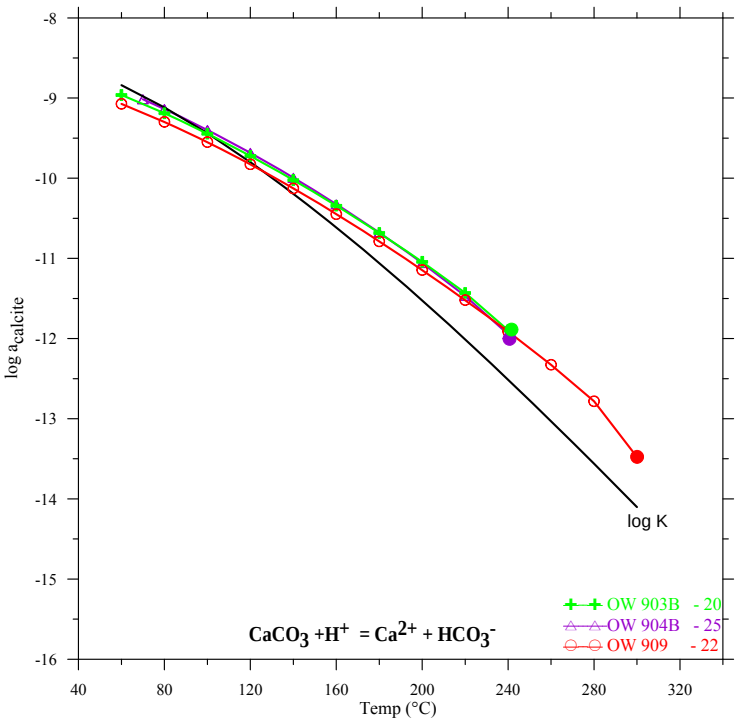


FIGURE 13: Calcite saturation during boiling of fluids from Olkaria Domes wells

## 6. CONCLUSIONS

- OW-909 seems to have higher concentrations of cation components than OW-903B and OW-904B. Despite the limited time of recovery, the sulphate concentrations are declining with time as the $H_2S$ concentrations increase, showing good geothermal water inflow into the wells.

- Solute and gas geothermometry indicate high temperatures in the range of 250-350°C.

- Olkaria Domes wells have a sodium bicarbonate water type and plot similar to those of Olkaria West and Olkaria Central fields, unlike the wells in the Olkaria East production field and in Olkaria Northeast, which discharge sodium-chloride type water of mature nature.

- With low calcium concentrations and high pH, calcite scaling can be expected to be minimal in these wells but fluid has to be separated at temperatures above 100°C to prevent silica scaling. There is also low carbon dioxide emission from these wells.

## ACKNOWLEDGEMENTS

I would like to extend my sincere gratitude to Dr. Ingvar B. Fridleifsson, the Director of the UNU Geothermal Training Programme for giving me the chance to take part in the Programme, and to the Deputy Director, Lúdvík S. Georgsson, for his ever present help; to Thórhildur Ísberg for her essential and valuable assistance during my stay in Iceland; and to Dorthe H. Holme and Markús A.G. Wilde for their expertise in making the studies and project work go easily.

My great and sincere appreciation to my supervisor Dr. Thráinn Fridriksson for his ever present guidance and hand in each page of this project paper, and for his wise counsel, encouragement and efficiency in the supervision of this project paper. To the UNU fellows who were always supportive and for the friendships forged. To the entire Orkustofnun community, thank you for all the assistance and support. I am grateful to my employer, Kenya Electricity Generating Company, for granting me this opportunity to come and pursue this course. A big thank you goes to Kizito Opondo for updating me with geochemical data. Thanks to my parents, Dr. and Mrs. W.O. Wanyanga, for their love, support and encouragement. Finally, thanks to God the Almighty for granting me wisdom and guidance.

## REFERENCES

Ármannsson, H. and Ólafsson, M., 2006: *Collection of geothermal fluids for chemical analysis*. Iceland GeoSurvey-ÍSOR, Reykjavík, report ISOR-2006/016, 17 pp.

Arnórsson S., 1998: *Interpretation of chemical and isotopic data on fluids discharged from wells in the Momotombo geothermal field with notes on gas chromatography analysis.* IAEA, project report NIC/8/008-05, 28 pp.

Arnórsson, S. and Bjarnason, J.Ó., 1994: *Icelandic Water Chemistry Group presents the chemical speciation programme WATCH Program upgrade: Version 2.1*. Science Institute, University of Iceland, Orkustofnun, Reykjavík, 7 pp.

Arnórsson, S. and Gunnlaugsson, E., 1983: Gas chemistry in geothermal systems. *Proceedings of the 9th Workshop on Geothermal Reservoir Engineering, Stanford University, Stanford, California*, 231-237.

Arnórsson, S., Gunnlaugsson, E., and Svavarsson, H., 1983: The chemistry of geothermal waters in Iceland II. Mineral equilibria and independent variables controlling water compositions. *Geochim. Cosmochim. Acta*, *47*, 547-566.

Clarke, M.C.G., Woodhall, D.G., Allen, D., and Darling, W.G., 1991: *Geological, volcanological and hydrogeological controls on the occurrence of geothermal activity in the area surrounding Lake Naivasha, Kenya.* Ministry of Energy, Nairobi, Kenya, report, 138 pp. + 3 maps.

D'Amore, F. and Arnórsson, S., 2000: Geothermometry. In: Arnórsson, S. (ed.), *Isotopic and chemical techniques in geothermal exploration, development and use. Sampling methods, data handling, and interpretation*. International Atomic Energy Agency, Vienna, 152-199.

D'Amore, F., and Celati, C., 1983: Methodology for calculating steam quality in geothermal reservoirs. *Geothermics, 12,* 129-140.

D'Amore, F., and Truesdell, A.H., 1985: Calculation of geothermal reservoir temperatures and steam fractions from gas compositions. *Geothermal Resources Council, Trans., 9*, 305-310.

Fournier, R.O., 1977: Chemical geothermometers and mixing model for geothermal systems. *Geothermics, 5,* 41-50.

Fournier, R.O., 1979: A revised equation for the Na/K geothermometer. *Geothermal Resources Council, Trans., 3,* 221-224.

Fournier, R.O. and Potter, R.W.II., 1982: A revised and expanded silica (quartz) geothermometer. *Geothermal Resources Council, Bull., 11-10,* 3-12.

Giggenbach, W.F., 1988: Geothermal solute equilibria. Derivation of Na-K-Mg-Ca geoindicators. *Geochim. Cosmochim. Acta, 52*, 2749-2765.

Giggenbach, W.F., 1991: Chemical techniques in geothermal exploration. In: D'Amore, F. (coordinator), *Application of geochemistry in geothermal reservoir development*. UNITAR/UNDP publication, Rome, 119-142.

Karingithi, C.W., 2000: Geochemical characteristics of the Greater Olkaria geothermal field, Kenya. Report 9 in: *Geothermal Training in Iceland 2000.* UNU-GTP, Iceland, 165-188.

Lagat, J.K., 2004: *Geology, hydrothermal alteration and fluid inclusion studies of the Olkaria Domes geothermal field, Kenya.* University of Iceland, MSc thesis, UNU-GTP, Iceland, report 2, 71 pp.

Moller, N., Greenberg, J.P., Weare, J.H., 2004: Computer modelling for geothermal systems: predicting carbonate and silica scale formation, $CO_2$ breakout and $H_2S$ exchange. *Transport in Porous Media Journal, 33-1/2,* 173-204.

Mungania, J., 1992: *Surface geology of Olkaria- Domes field*. Kenya Power Company, unpublished internal report.

Mungania, J., 1999: *Reservoir model of Olkaria-Domes field*. KenGen, unpublished internal report.

Ocampo-Díaz, J.D., Núñez, Q.M., Moya-Acosta, S.L., 2005: Silica scaling as a predominant factor of the production in Cerro Prieto geothermal wells, Mexico. *Proceedings of the World Geothermal Congress 2005, Anatalya, Turkey*, CD, 5 pp.

Omenda, P.O., 1999: *Borehole geology of well OW-901*. KenGen, unpublished internal report.

Onacha, S.A., 1993: *Resistivity survey of Olkaria-Domes field*. Kenya Power Company, unpublished internal report.

Onacha, S.A., and Mungania, J., 1993: Surface exploration of Domes Area: An extension of Olkaria geothermal field. *Proceedings of the 14th New Zealand Geothermal Proceedings, Auckland, NZ*, 6 pp.

Opondo, 2007: *Corrosive species and scaling in wells at Olkaria and Reykjanes, Svartsengi and Nesjavellir, Iceland.* University of Iceland, MSc thesis, UNU-GTP, Iceland, report 2, 76 pp.

Opondo, K.M., 2008: Fluid characteristics of three exploration wells drilled at Olkaria Domes field, Kenya. *Proceedings of the 33rd Workshop on Geothermal Reservoir Engineering, Stanford University, Stanford, Ca*, 6 pp.

Pang Z.H., and Ármannsson, H. (editors), 2006*: Analytical procedures and quality assurance for geothermal water chemistry*. UNU-GTP, Iceland, Report 1, 172 pp.

Stapleton, M., 2002: *Scaling and corrosion in geothermal operation*. GeoChemical Services - PowerChem Technology, 7 pp.

Tole, M.P., Ármannsson, H., Pang Z.H., and Arnórsson, S., 1993: Fluid/mineral equilibrium calculations for geothermal fluids and chemical geothermometry. *Geothermics, 22*, 17-37.

## APPENDIX I: Water and gas analysis and deep fluid concentrations in the Olkaria Domes wells

TABLE 1: Deep fluid concentration

| Well/Sample No. | pH | B | $SiO_2$ | Na | K | Mg | Ca | F | Cl | $SO_4$ | TDS | $CO_2$ | $H_2S$ | $H_2$ | $CH_4$ | $N_2$ |
|---|---|---|---|---|---|---|---|---|---|---|---|---|---|---|---|---|
| 903B - 13 | 7.0 | 0.7 | 176.2 | 402.8 | 66.2 | 0.0 | 1.1 | 46.9 | 149.1 | 314.5 | 1021.7 | 1239.6 | 1.7 | 0.1 | 2.3 | 38.1 |
| 903B - 18 | 7.5 | 0.6 | 198.0 | 505.2 | 38.8 | 0.5 | 1.3 | 29.6 | 138.8 | 505.9 | 979.4 | 585.9 | 0.8 | 2.5 | 7.9 | 0.0 |
| 903B - 20 | 7.7 | 1.9 | 457.3 | 446.7 | 74.7 | 0.0 | 0.2 | 52.8 | 177.6 | 234.6 | 1048.4 | 592.2 | 9.2 | 2.2 | 0.1 | 0.7 |
| 903B - 21 | 7.8 | 1.6 | 351.6 | 442.5 | 89.5 | 0.0 | 0.4 | 56.4 | 147.3 | 215.6 | 1021.7 | 580.8 | 25.4 | 1.4 | 0.1 | 0.5 |
| 904B - 11 | 7.2 | 1.4 | 424.0 | 292.4 | 35.5 | 0.0 | 2.1 | 42.3 | 141.3 | 109.3 | 689.6 | 991.3 | 5.0 | 0.4 | 3.0 | 85.4 |
| 904B - 12 | 6.9 | 0.1 | 426.8 | 339.9 | 30.5 | 0.0 | 1.6 | 41.4 | 122.0 | 293.3 | 777.7 | 1510.0 | 2.6 | 0.4 | 3.2 | 120.1 |
| 904B - 16 | 7.0 | 0.8 | 119.5 | 327.7 | 38.8 | 0.0 | 1.0 | 39.4 | 148.0 | 189.5 | 816.6 | 1443.9 | 1.5 | 2.3 | 0.3 | 10.4 |
| 904B - 19 | 7.4 | 1.4 | 381.7 | 332.7 | 41.2 | 0.0 | 0.6 | 37.1 | 164.2 | 166.7 | 818.7 | 792.2 | 5.7 | 0.2 | 0.6 | 0.0 |
| 904B - 24 | 7.1 | 1.3 | 517.6 | 310.7 | 360.6 | 0.0 | 0.6 | 36.3 | 170.0 | 142.0 | 807.1 | 2321.9 | 22.5 | 0.5 | 1.0 | 34.1 |
| 904B - 25 | 7.3 | 1.9 | 327.1 | 338.1 | 97.3 | 0.0 | 0.2 | 36.9 | 169.3 | 131.9 | 780.5 | 1191.7 | 21.0 | 0.6 | 1.4 | 29.2 |
| 909 - 12 | 7.3 | 1.9 | 352.7 | 562.8 | 159.2 | 0.0 | 0.1 | 155.6 | 473.9 | 68.8 | 1179.0 | 1962.3 | 1.8 | 2.9 | 0.1 | 2.2 |
| 909 - 15 | 7.4 | 1.5 | 478.9 | 560.4 | 211.0 | 0.0 | 0.1 | 156.0 | 479.0 | 66.3 | 1179.5 | 2188.3 | 0.6 | 5.6 | 1.7 | 78.4 |
| 909 - 17 | 8.0 | 3.5 | 408.7 | 532.7 | 229.1 | 0.0 | 0.1 | 144.4 | 477.8 | 52.0 | 1390.6 | 718.1 | 0.7 | 0.4 | 0.9 | 40.3 |
| 909 - 20 | 8.3 | 3.4 | 453.5 | 527.0 | 233.8 | 0.0 | 0.2 | 139.6 | 402.5 | 36.9 | 2211.5 | 624.8 | 4.9 | 2.6 | 1.4 | 7.9 |
| 909 - 22 | 7.8 | 2.7 | 294.9 | 537.5 | 224.3 | 0.0 | 0.1 | 153.2 | 484.9 | 27.7 | 1532.1 | 912.3 | 8.6 | 0.3 | 0.7 | 30.0 |
| 909 - 26 | 7.9 | 2.8 | 261.3 | 574.5 | 214.2 | 0.0 | 0.2 | 136.0 | 493.2 | 24.5 | 696.5 | 609.1 | 10.7 | 2.8 | 3.7 | 90.6 |

TABLE 2: Water and gas analysis of fluids from well OW-903B

| | | | | | | OW 903B Water Analysis (ppm) | | | | | | | | | | | | | | | Gas Analysis (ppm) | | | | |
|---|---|---|---|---|---|---|---|---|---|---|---|---|---|---|---|---|---|---|---|---|---|---|---|---|
| Day | GSP (bar) | WHP (bar) | Temp (°C) | Enth. kJ/kg | Cond | TDS (ppm) | pH | B | $SO_4$ | Cl | $CO_2$ | F | $H_2S$ | $SiO_2$ | Ca | Li | Na | K | Mg | $CO_2$ | $H_2S$ | $CH_4$ | $H_2$ | $N_2$ |
| 1 | 2.1 | 3.8 | 94.0 | 1307 | 2776 | 1390 | 9.5 | 0.9 | 717.7 | 196.7 | 266.2 | 41.6 | 0.1 | 281.3 | | 1.5 | 512.6 | 55.1 | 0.7 | 4382 | 9.2 | 15.8 | | 418 |
| 2 | 2.3 | 3.8 | 90.0 | 1325 | 2924 | 1462 | 9.4 | 0.1 | 699.0 | 175.7 | 225.3 | 46.5 | 0.3 | | | 1.4 | 482.3 | 61.6 | 0.2 | | 3.2 | 15.0 | 0.2 | 2033 |
| 3 | | 4.0 | 94.5 | 1466 | 2740 | 1368 | 8.7 | 1.7 | 677.6 | 178.2 | 436.7 | 45.6 | 0.2 | 285.3 | | | 549.6 | 71.6 | | 4580 | 4.0 | 27.6 | 0.2 | 1980 |
| 9 | | 4.0 | 90.0 | 1516 | 2310 | 1156 | 9.6 | 1.8 | | 202.0 | 243.3 | 43.8 | 1.2 | 287.5 | 0.0 | 1.4 | 498.5 | 83.8 | | 5091 | 11.9 | 41.8 | | 1273 |
| 10 | 2.3 | 3.8 | 89.5 | 1425 | 2967 | 1481 | 9.6 | 0.1 | 679.4 | 189.6 | 290.4 | 58.0 | 1.0 | 184.5 | 3.6 | 1.4 | 589.2 | 80.8 | | 6189 | 2.8 | 0.2 | | 16 |
| 13 | 1.8 | 3.6 | 89.0 | 1567 | 2954 | 1490 | 10.2 | 0.6 | 497.2 | 201.6 | 341.0 | 50.4 | 1.7 | 251.8 | 8.3 | 1.2 | 538.4 | 90.7 | | 5221 | 42.4 | 8.0 | 0.3 | 764 |
| 14 | 1.2 | 3.6 | 92.0 | 1595 | 2968 | 1525 | 9.5 | 0.7 | 472.2 | 203.1 | 385.9 | 55.8 | 1.4 | | 0.7 | 1.2 | 564.7 | 82.8 | | 8080 | 5.5 | 5.6 | 0.2 | 452 |
| 15 | 3.4 | 5.2 | 89.0 | 1461 | 2993 | 1497 | 9.6 | 0.9 | 639.4 | 199.5 | 281.1 | 51.2 | 3.4 | 266.3 | | 1.6 | 535.8 | 94.8 | | 5227 | 9.4 | 18.9 | 1.8 | 1603 |
| 16 | 3.7 | 5.7 | 85.0 | 1434 | 2942 | 1471 | 9.5 | 1.0 | 708.1 | 224.7 | 303.4 | 60.4 | 0.7 | 413.0 | | 1.4 | 513.3 | 92.2 | | | 1.3 | 9.8 | 0.9 | 678 |
| 17 | 4.1 | 7.5 | 84.1 | 1334 | 2870 | 1431 | 10.1 | 0.8 | 655.2 | 195.6 | 330.0 | 50.0 | 2.4 | | 0.1 | 1.1 | 482.7 | 49.7 | | | 7.2 | 9.5 | 0.9 | 664 |
| 20 | 4.1 | 7.6 | 86.0 | 1253 | 2897 | 1422 | 9.4 | 0.7 | 624.8 | 202.4 | 338.4 | 64.0 | 0.5 | 585.0 | 1.6 | 1.2 | 411.5 | 87.0 | | 5753 | 7.0 | 7.0 | 0.7 | 469 |
| 21 | 3.8 | 7.9 | | 1453 | 2897 | 1442 | 9.6 | 0.2 | 538.2 | 220.8 | 280.5 | 53.8 | 1.0 | 273.5 | 1.6 | 1.5 | 431.9 | 0.0 | | | | | | |
| 24 | 4.1 | 7.6 | 85.0 | 1247 | 2880 | 1450 | 9.2 | 1.0 | 446.4 | 211.6 | 274.2 | 66.5 | 1.2 | 250.0 | 1.5 | 1.5 | 571.7 | 94.0 | | 12788 | 10.9 | 27.6 | 0.7 | 465 |
| 30 | 4.1 | 7.2 | 88.0 | | | | | | 380.8 | | | | | | 7.2 | | | 0.0 | | | | | | |
| 35 | 3.8 | 5.9 | 93.0 | 1007 | | | 10.2 | 0.4 | 481.1 | 224.0 | 273.5 | 79.0 | 0.7 | 304.5 | 1.5 | | 526.5 | 105.1 | | 6665 | 11.3 | 1.3 | 0.4 | 480 |
| 43 | 3.4 | 5.6 | | 1916 | 2966 | 1483 | 10.1 | 1.3 | 418.0 | 220.0 | 322.3 | 67.5 | 0.9 | 677.0 | 1.0 | 2.9 | 533.0 | 112.1 | | 11275 | 2.4 | 4.9 | 42.6 | 17 |
| 50 | 3.4 | 4.8 | | 1591 | 2954 | 1477 | 9.5 | 1.3 | 310.0 | 243.0 | 351.1 | 73.0 | 0.7 | 627.0 | 1.0 | 1.2 | 483.1 | 95.7 | | 14197 | 2.3 | 2.7 | | 12 |
| 58 | 2.1 | 3.8 | | 1307 | 2775 | 1390 | 9.5 | 0.9 | 718.0 | 197.0 | 317.0 | 42.0 | 0.1 | 281.0 | 1.9 | 1.5 | 717.0 | 55.0 | 0.7 | 4383 | 9.3 | 95.6 | 29.8 | |
| 62 | 3.9 | 6.2 | | 1490 | 2887 | 1444 | 10.3 | 2.2 | 336.0 | 252.0 | 348.0 | 82.0 | 1.9 | 621.0 | 1.2 | 1.2 | 614.0 | 124.0 | | 3396 | 33.4 | 1.5 | 26.2 | 9 |
| 64 | 4.1 | 6.3 | | 1414 | 2980 | 1488 | 9.4 | 2.7 | 333.0 | 252.0 | 359.0 | 75.0 | 1.5 | 649.0 | 0.3 | 1.9 | 634.0 | 106.0 | | 4146 | 99.9 | 1.8 | 26.3 | 9 |
| 70 | 3.4 | 6.2 | | 1638 | 2880 | 1450 | 9.6 | 2.3 | 306.0 | 209.0 | 365.0 | 80.0 | 4.8 | 499.0 | 0.6 | 2.8 | 628.0 | 127.0 | | 3941 | 267.7 | 1.1 | 16.8 | 6 |
| 72 | 4.6 | 8.3 | | 1487 | 2906 | 1455 | 9.7 | 2.5 | 350.0 | 281.0 | 383.0 | 59.0 | 4.8 | 587.0 | 0.1 | 0.1 | 613.0 | 138.0 | | 4292 | 144.6 | 0.9 | 16.9 | |
| 79 | 4.1 | 8.1 | | 1535 | 2945 | 1472 | 9.9 | 2.3 | 323.0 | 262.0 | 362.0 | 77.0 | 5.0 | 449.0 | 0.2 | 4.7 | 612.0 | 124.0 | | 4229 | 29.1 | 4.4 | 39.4 | 8 |
| 84 | 5.5 | 10.3 | | 1466 | 2842 | 1421 | 10.1 | 2.2 | 310.0 | 267.0 | 374.0 | 62.0 | | 726.0 | 0.3 | 2.6 | 612.0 | 129.0 | | 9604 | 120.6 | 2.8 | 16.0 | 7 |
| 86 | 2.8 | 10.3 | | 1488 | 2902 | 1451 | 9.9 | 2.0 | 278.0 | 587.0 | 360.0 | 61.0 | 5.8 | 623.0 | 1.2 | 0.2 | 620.0 | 139.0 | | 10134 | 32.2 | 3.4 | 22.3 | 10 |

TABLE 3: Water and gas analysis of fluids from well OW-904B

| | | | | | OW 904B Water Analysis (ppm) | | | | | | | | | | | | | | | | Gas Analysis (ppm) | | | | |
|---|---|---|---|---|---|---|---|---|---|---|---|---|---|---|---|---|---|---|---|---|---|---|---|---|---|
| Day | GSP (bar) | WHP (bar) | Temp (°C) | Enth. (kJ/kg) | Cond | TDS (ppm) | pH | B | $SO_4$ | Cl | $CO_2$ | F | $H_2S$ | $SiO_2$ | Ca | Li | Na | K | Mg | $CO_2$ | $H_2S$ | $CH_4$ | $H_2$ | $N_2$ |
| 1 | 2.1 | 3.2 | 94.0 | 1307 | 2222 | 1106 | 6.0 | | 782.5 | 124.3 | | 36.8 | 3.4 | 212.0 | | 0.4 | 322.0 | 52.9 | 0.5 | | 3.4 | | | |
| 3 | 3.6 | 7.9 | 87.0 | 1325 | 2183 | 1092 | 5.7 | 1.4 | 686.1 | 124.6 | | 48.9 | 0.4 | 106.5 | | 0.5 | 298.5 | 19.2 | 0.5 | 9166.2 | 8.6 | 45.0 | 2.4 | 3570 |
| 4 | 2.4 | 4.0 | 90.0 | 1466 | 2090 | 1045 | 5.9 | 1.0 | 732.2 | 133.5 | 172.6 | 49.1 | 0.2 | 238.8 | | | 359.0 | 48.4 | | 10033.9 | 6.4 | 20.7 | 2.3 | 869 |
| 10 | 2.4 | 5.0 | 90.0 | 1516 | 3085 | 1540 | 8.8 | 0.9 | 591.2 | 177.1 | | 49.4 | 0.2 | 207.7 | 3.4 | 0.8 | 347.3 | 46.3 | | 8719.4 | 36.7 | 143.1 | 1.4 | 420 |
| 14 | 2.8 | 4.6 | 89.0 | 1567 | 2061 | 1037 | 9.7 | 0.9 | 401.6 | 168.3 | 337.9 | 61.8 | 0.8 | 285.7 | 1.1 | 0.6 | 350.7 | 42.4 | | 8247.7 | 2.1 | 14.5 | 6.3 | 984 |
| 15 | 2.8 | 4.9 | 89.0 | 1595 | 2275 | 1137 | 9.1 | 1.0 | 515.3 | 182.8 | 171.6 | 51.8 | 1.4 | 0.0 | 2.0 | 0.9 | 434.3 | 45.0 | | 21770.2 | 1.9 | 19.5 | 7.3 | 1090 |
| 16 | 4.4 | 6.5 | 83.0 | 1461 | 2286 | 1143 | 9.2 | 0.3 | 562.9 | 198.8 | 124.9 | 50.1 | 3.4 | 243.0 | | 0.9 | 446.2 | 47.3 | | 13083.5 | 13.0 | 29.4 | 3.7 | 1042 |
| 17 | 5.1 | 6.5 | 81.3 | 1434 | 2253 | 1126 | 9.2 | 0.5 | 556.1 | 203.8 | 171.8 | 59.1 | 0.5 | 326.0 | | 0.8 | 419.4 | 45.0 | | 4359.2 | 8.2 | 37.0 | 4.6 | 1270 |
| 18 | 5.0 | 6.9 | 85.0 | 1334 | 2259 | 1129 | 10.0 | 0.1 | 647.2 | 192.8 | 255.4 | 52.2 | 0.3 | | 1.0 | 0.4 | 413.9 | 47.2 | | 21677.2 | 26.5 | 32.7 | 3.7 | 1051 |
| 21 | 5.0 | 6.7 | 84.0 | 1253 | 2203 | 1102 | 9.4 | 1.0 | 524.1 | 198.4 | | 52.3 | 0.3 | 546.0 | 1.8 | 1.0 | 350.6 | 46.6 | | 10420.8 | 5.8 | 34.4 | 3.9 | 1094 |
| 24 | 4.5 | 6.7 | 84.0 | 1471 | 2031 | 1010 | 9.6 | 2.0 | 160.0 | 207.0 | 144.6 | 62.0 | 5.8 | 621.0 | 3.1 | | 428.2 | 52.0 | | 8993.4 | 15.6 | 29.9 | 3.8 | 846 |
| 25 | 5.1 | 6.9 | 85.0 | 1525 | 2271 | 1139 | 9.4 | 0.2 | 429.6 | 178.6 | 156.9 | 60.6 | 2.2 | 625.0 | 2.3 | 0.5 | 497.8 | 44.6 | | 14064.8 | 13.5 | 31.5 | 4.3 | 1190 |
| 31 | 5.0 | 6.5 | | | 2894 | 1138 | 9.5 | 0.2 | 381.2 | 200.6 | 199.3 | 55.3 | | 247.5 | 2.8 | | 408.1 | 49.8 | | 199.3 | | | | |
| 36 | 3.6 | 5.4 | | 1676 | | | 10.0 | 1.5 | 414.0 | 213.0 | 197.6 | 50.8 | 1.4 | 220.0 | 0.2 | | 421.9 | 48.5 | | 9524.7 | 8.9 | 3.5 | 10.3 | 362 |
| 44 | 3.5 | 6.2 | | 1560 | 2366 | 1183 | 9.7 | 2.1 | 289.6 | 209.5 | 237.6 | 57.6 | 1.3 | 516.0 | 1.0 | 1.4 | 426.2 | 51.1 | | 12242.8 | 120.6 | 3.8 | 20.7 | 136 |
| 51 | 4.1 | 5.2 | | 2178 | 2390 | 1196 | 9.7 | 1.2 | 277.5 | 216.7 | 265.5 | 57.7 | 1.4 | 175.0 | 1.4 | 1.3 | 479.9 | 56.8 | | 12744.0 | 6.3 | 3.4 | 23.0 | 103 |
| 58 | 3.5 | 7.6 | | 1824 | 2350 | 1181 | 9.6 | 2.7 | 278.4 | 226.4 | 330.0 | 73.5 | 1.4 | 420.0 | 1.0 | 1.2 | 500.1 | 64.0 | | 7937.5 | 2.5 | 3.0 | 22.2 | 311 |
| 63 | 3.9 | 7.6 | | 2009 | 2341 | 1169 | 10.3 | 2.4 | 241.4 | 240.2 | 253.0 | 54.0 | 2.8 | 492.0 | 0.6 | 1.2 | 489.6 | 62.6 | | 6457.8 | 74.6 | 6.8 | 3.4 | 337 |
| 65 | 4.3 | 7.2 | | 2043 | 2376 | 1199 | 9.4 | 2.0 | 244.2 | 240.5 | 276.5 | 54.3 | 4.8 | 559.0 | 0.9 | 1.2 | 487.3 | 60.3 | | 6239.5 | 28.3 | 6.3 | 2.3 | |
| 71 | 6.9 | 9.7 | | 1535 | 2062 | 1029 | 9.8 | 2.1 | 217.9 | 186.7 | 290.8 | 50.6 | 8.2 | 446.0 | 0.7 | 1.1 | 460.8 | 78.3 | | 5631.2 | 164.9 | 7.8 | 2.3 | 370 |
| 73 | 7.6 | 10.3 | | 1690 | 2386 | 1193 | 9.7 | 1.7 | 232.4 | 255.0 | 294.4 | 53.5 | 8.1 | 677.0 | 0.7 | 0.9 | 454.9 | 71.8 | | 7735.4 | 135.6 | 6.9 | 2.2 | 331 |
| 80 | 5.4 | 10.3 | | 1481 | 2380 | 1190 | 10.0 | 1.8 | 214.7 | 227.0 | 262.9 | 57.9 | 9.5 | 502.0 | 0.7 | 1.1 | 457.3 | 76.7 | | 9417.7 | 77.7 | 5.1 | 2.0 | 321 |
| 85 | 5.5 | 17.9 | | 1812 | 2295 | 1147 | 10.2 | 2.0 | 189.1 | 231.3 | 290.2 | 54.4 | 8.5 | 652.0 | 1.1 | 1.2 | 459.1 | 87.6 | | 12540.6 | 271.1 | 13.5 | 5.7 | 283 |
| 87 | 5.2 | 17.9 | | 2168 | 2366 | 1182 | 9.9 | 1.9 | 208.0 | 249.0 | 275.9 | 53.2 | 7.8 | 758.0 | 0.8 | 1.1 | 455.0 | 128.1 | | 21427.9 | 177.9 | 10.4 | 5.3 | 338 |
| 92 | 5.5 | 17.0 | | 1924 | 2287 | 1143 | 9.7 | 2.8 | 193.1 | 247.9 | 286.9 | 54.1 | 8.2 | 479.0 | 0.3 | 1.1 | 495.1 | 142.5 | | 10159.5 | 160.7 | 13.7 | 6.3 | 289 |
| 94 | 2.9 | 17.9 | | 1857 | 2298 | 1140 | 9.6 | 3.0 | 206.5 | 303.6 | 278.1 | 52.9 | 6.9 | 473.0 | 1.4 | 1.2 | 455.9 | 131.1 | | 8395.8 | 210.7 | 16.0 | 8.8 | 851 |

TABLE 4: Water and gas analysis of fluids from well OW-909

| | | | | | | OW 909 Water Analysis (ppm) | | | | | | | | | | | | | | | | Gas Analysis (ppm) | | | | |
|---|---|---|---|---|---|---|---|---|---|---|---|---|---|---|---|---|---|---|---|---|---|---|---|---|---|---|
| Day | GSP (bar) | WHP (bar) | Temp (°C) | Enth. (kJ/kg) | Cond | TDS (ppm) | pH | B | $SO_4$ | Cl | $CO_2$ | F | $H_2S$ | $SiO_2$ | Ca | Li | Na | K | Mg | $CO_2$ | $H_2S$ | $CH_4$ | $H_2$ | $N_2$ |
| 1 | 3.7 | 2.8 | 86.0 | 1552.0 | 3910 | 2737 | 9.6 | 0.08 | 177.3 | 652.8 | 294.4 | 229.0 | 0.34 | 358.0 | 1.60 | 0.358 | 779.0 | 215.7 | nd | 8710.2 | 5.4 | | 1.1 | 3188 |
| 5 | 3.1 | 6.2 | 89.0 | 2001.0 | 4000 | 2800 | 10.1 | 0.58 | 250.3 | 732.4 | 203.1 | 250.0 | 0.95 | 530.0 | 2.60 | 0.364 | 641.7 | | nd | 11302.9 | 2.8 | 2.3 | 12.3 | 380 |
| 8 | 2.9 | 6.9 | 86.0 | 1697.0 | 3999 | 2000 | 9.9 | 0.12 | 152.6 | 743.4 | 162.8 | 284.9 | 1.36 | 395.0 | 6.61 | 0.322 | 732.4 | 222.5 | nd | 162.8 | 1.4 | | | |
| 9 | 3.4 | 6.5 | 90.0 | 1875.0 | 4230 | 2961 | 9.4 | 0.43 | 179.8 | 765.7 | 202.8 | 323.6 | 1.16 | 652.0 | 0.35 | 0.358 | 852.9 | 255.5 | nd | 3983.4 | 5.5 | 1.0 | 15.9 | 224 |
| 14 | 3.4 | 6.2 | | 1904.0 | 4350 | 3045 | 10.0 | 0.97 | 85.0 | 772.3 | 275.7 | 310.7 | 0.34 | 436.5 | 0.35 | 1.946 | 770.0 | 270.7 | nd | 5386.6 | 0.9 | 1.2 | 29.6 | 414 |
| 16 | 3.4 | 7.0 | | 1783.0 | 4430 | 3101 | 9.8 | 0.61 | 109.4 | 875.4 | 255.4 | 305.5 | 0.48 | 441.0 | 0.10 | 0.336 | 869.1 | 274.2 | nd | 4116.5 | 2.7 | 1.3 | 26.9 | 376 |
| 19 | 2.2 | 3.6 | | 1831.0 | 4450 | 3115 | 10.0 | | | 827.9 | 230.6 | 235.0 | 0.34 | 943.0 | 0.31 | 0.388 | 900.0 | 260.4 | nd | 9347.8 | 5.6 | | | |
| 21 | 3.5 | 7.0 | | 1696.0 | 5420 | 2711 | 10.3 | 2.86 | 81.2 | 817.6 | 179.1 | 292.4 | 0.71 | 932.0 | 0.23 | 2.833 | 850.8 | 304.3 | nd | 13494.2 | 12.5 | 1.8 | 32.9 | 68 |
| 22 | 3.5 | 7.0 | | 1990.0 | 5032 | 2516 | 10.0 | 2.70 | 69.9 | 786.6 | 218.7 | 257.4 | | 898.0 | 0.20 | 2.033 | 913.4 | 287.4 | nd | 6479.0 | 7.0 | 1.1 | 28.9 | 32 |
| 23 | 3.0 | 7.0 | | 2220.0 | 6168 | 3100 | 10.1 | 2.17 | 95.8 | 803.7 | 261.6 | 191.9 | | 738.0 | 0.20 | 2.821 | 905.8 | 280.2 | nd | 13937.0 | 4.9 | 1.0 | 24.9 | 23 |
| 26 | 3.1 | 7.0 | | 2051.0 | 2223 | 1104 | 10.0 | 1.60 | 132.3 | 780.5 | 255.0 | 287.8 | 0.51 | 950.0 | 0.54 | 1.072 | 909.3 | 286.0 | nd | 8735.3 | 12.0 | 1.0 | 27.0 | 31 |
| 27 | 3.5 | 6.3 | | 2015.0 | 3999 | 2000 | 9.6 | 3.28 | 116.7 | 803.6 | 226.8 | 263.9 | 0.68 | 598.0 | 0.14 | 0.38 | 954.4 | 270.0 | nd | 12924.5 | 10.6 | 0.7 | 20.0 | 15 |
| 28 | 3.5 | 6.3 | | 2070.0 | 4972 | 2486 | 10.0 | 3.88 | 116.6 | 806.8 | 248.2 | 249.0 | 0.48 | 664.0 | 0.17 | 2.71 | 954.0 | 274.6 | nd | 7409.8 | 4.8 | 1.1 | 20.6 | 248 |
| 29 | 3.3 | 6.3 | | 2050.0 | 2316 | 1155 | 10.0 | 3.45 | 115.6 | 822.0 | 230.6 | 261.7 | 0.31 | 831.0 | 0.23 | 2.066 | 962.6 | 374.6 | nd | 5364.8 | 3.5 | 9.8 | 3.6 | 413 |
| 30 | 4.0 | 7.0 | | 2028.0 | 4480 | 2000 | 9.8 | 2.52 | 112.5 | 812.3 | 266.9 | 264.5 | 0.75 | 812.0 | 0.14 | 0.23 | 950.2 | 357.8 | nd | 14369.4 | 2.1 | 12.1 | 38.9 | 545 |
| 33 | 3.9 | 6.9 | | 2029.0 | 4490 | 2000 | 10.0 | 2.65 | 114.2 | 810.9 | 289.7 | 250.7 | 0.68 | 760.0 | 0.14 | 6.62 | 939.2 | 398.3 | nd | 2937.6 | 6.0 | 6.4 | 3.0 | 285 |
| 35 | 3.7 | 6.9 | | 1955.0 | 4712 | 2358 | 9.9 | 5.94 | 88.2 | 810.2 | 232.3 | 244.9 | 0.68 | 693.0 | 0.18 | 6.09 | 903.3 | 388.5 | nd | 4255.7 | 2.4 | 6.2 | 2.6 | 279 |
| 40 | 3.5 | 5.7 | | 2273.0 | 5348 | 2674 | 10.6 | 3.30 | 83.7 | 816.1 | 202.2 | 270.3 | 0.85 | 950.0 | 0.11 | 2.231 | 925.5 | 360.3 | nd | 7665.0 | 21.8 | 5.5 | 0.4 | 449 |
| 42 | 3.5 | 6.5 | | 1834.0 | 5858 | 2929 | 10.3 | 4.74 | 82.4 | 849.2 | 216.7 | 287.1 | 2.38 | 645.0 | 0.16 | 0.02 | 909.6 | 373.1 | nd | 3572.9 | 287.5 | 9.6 | 3.8 | 282 |
| 48 | 3.2 | 6.6 | | 2089.0 | 9750 | 3750 | 10.1 | 5.80 | 62.6 | 682.5 | 294.1 | 236.7 | 0.94 | 769.0 | 0.33 | 6.19 | 893.6 | 396.5 | nd | 3393.2 | 30.4 | 9.6 | 18.1 | 54 |
| 50 | 3.3 | 6.5 | | 2065.0 | 5360 | 2690 | 10.0 | 4.12 | 46.1 | 847.1 | 280.3 | 263.9 | 3.06 | 965.0 | 0.15 | 7.27 | 863.9 | 387.6 | nd | 3483.6 | 22.1 | 7.5 | 3.3 | 214 |
| 57 | 4.1 | 7.9 | | 1985.0 | 5192 | 2598 | 10.2 | 4.58 | 46.9 | 822.2 | 183.5 | 259.7 | 3.03 | 500.0 | 0.20 | 2.004 | 911.0 | 380.4 | nd | 5725.9 | 50.0 | 5.1 | 2.3 | 209 |
| 62 | 4.1 | 8.0 | | 1993.0 | 4656 | 2328 | 10.3 | 2.21 | 51.6 | 843.0 | 265.0 | 273.2 | 1.22 | 886.0 | 0.09 | 1.32 | 912.1 | 434.1 | nd | 4840.7 | 55.8 | 8.8 | 6.2 | 162 |
| 64 | 5.2 | 8.1 | | 1991.0 | 4825 | 2420 | 10.2 | 4.70 | 42.7 | 719.5 | 286.2 | 272.0 | 3.40 | 926.0 | 0.10 | 5.97 | 892.9 | 340.2 | nd | 8309.6 | 53.1 | 8.9 | 6.0 | 133 |
| 69 | 4.5 | 8.3 | | 2016.0 | 4794 | 2398 | 10.0 | 4.96 | 38.9 | 872.7 | 222.4 | 289.8 | 3.40 | 835.0 | 0.72 | 2.781 | 951.6 | 281.5 | nd | 4851.9 | 7.7 | 12.0 | 7.8 | 87 |
| 71 | 2.6 | 8.5 | | 2235.0 | 2364 | 1181 | 9.8 | 4.66 | 41.6 | 836.4 | 245.7 | 230.7 | 3.40 | 443.0 | 0.29 | 1.088 | 974.1 | 363.2 | nd | 3441.6 | 63.1 | 25.5 | 19.2 | 623 |
| 78 | 1.8 | 8.4 | | 2150.0 | 5175 | 2550 | 9.9 | 4.56 | 25.8 | 836.4 | 251.7 | 226.0 | 3.40 | 569.0 | | 1.418 | 942.7 | 165.3 | nd | 4761.6 | 58.9 | 0.9 | 2.0 | 115 |
| 84 | 3.1 | 8.5 | | 1996.0 | 4524 | 2260 | 10.5 | 4.57 | 47.4 | 936.0 | 184.4 | 230.2 | 3.40 | 716.0 | | 2.729 | 1047.0 | | nd | 3942.0 | 72.3 | 13.4 | 3.5 | 674 |
| 85 | 3.7 | 8.4 | | 2153.0 | 3243 | 1623 | 10.1 | 4.13 | 26.0 | 853.7 | 237.8 | 263.2 | 2.96 | 746.0 | | 2.699 | 1003.0 | | nd | 6011.4 | 31.6 | 16.6 | 6.3 | 113 |
| 90 | 7.0 | 10.4 | | 2168.0 | 5302 | 2651 | 10.6 | 4.33 | 47.2 | 848.9 | 170.9 | 257.9 | 2.86 | 884.0 | | 2.878 | 995.0 | | nd | 6672.4 | 46.2 | 9.0 | 3.9 | 84 |
| 92 | 4.8 | 10.0 | | 2219.0 | 4364 | 2680 | 9.9 | 4.66 | | 591.3 | 199.3 | 235.0 | 3.67 | 725.0 | | 2.996 | 1056.0 | | nd | 5314.3 | 74.6 | 2.9 | 1.3 | 165 |
| 97 | | | | | 5378 | 2689 | 10.3 | 3.26 | 50.7 | 824.7 | 244.0 | 244.0 | 2.72 | 512.0 | | 2.872 | 807.5 | | nd | 4780.6 | 61.6 | 0.2 | 0.5 | 88 |
| 104 | 5.4 | 14.3 | | 1527.0 | 6420 | 3210 | 10.7 | 3.37 | 7.7 | 545.3 | 213.0 | 305.2 | 2.82 | 831.0 | | 2.982 | 734.0 | | nd | 6163.2 | 38.1 | 1.1 | 2.5 | 267 |
| 106 | 4.8 | 14.3 | | 2072.0 | 4320 | 2200 | 10.5 | 3.83 | 24.5 | 545.3 | 192.1 | 260.9 | 2.99 | 583.0 | | 2.94 | 1040.0 | | nd | 4186.4 | 14.9 | | | 132 |
| 112 | 5.2 | 23.1 | | 1872.0 | 4980 | 2490 | 11.0 | 3.66 | 27.5 | 812.1 | 165.2 | 307.6 | 2.38 | 703.0 | | 2.951 | | | nd | 165.2 | 2.4 | | | |
| 118 | | | | 1994.0 | | | 11.0 | 3.81 | 21.3 | 799.2 | 147.4 | 255.6 | | 560.0 | | 2.964 | | | nd | 147.4 | | | | |
| 121 | 1.7 | 7.2 | | 1232.0 | | | 10.9 | | | | | | | | | | | | nd | | | | | |

*nd - not detectable

## APPENDIX II: Chemical trends in the discharge of the Olkaria Domes wells

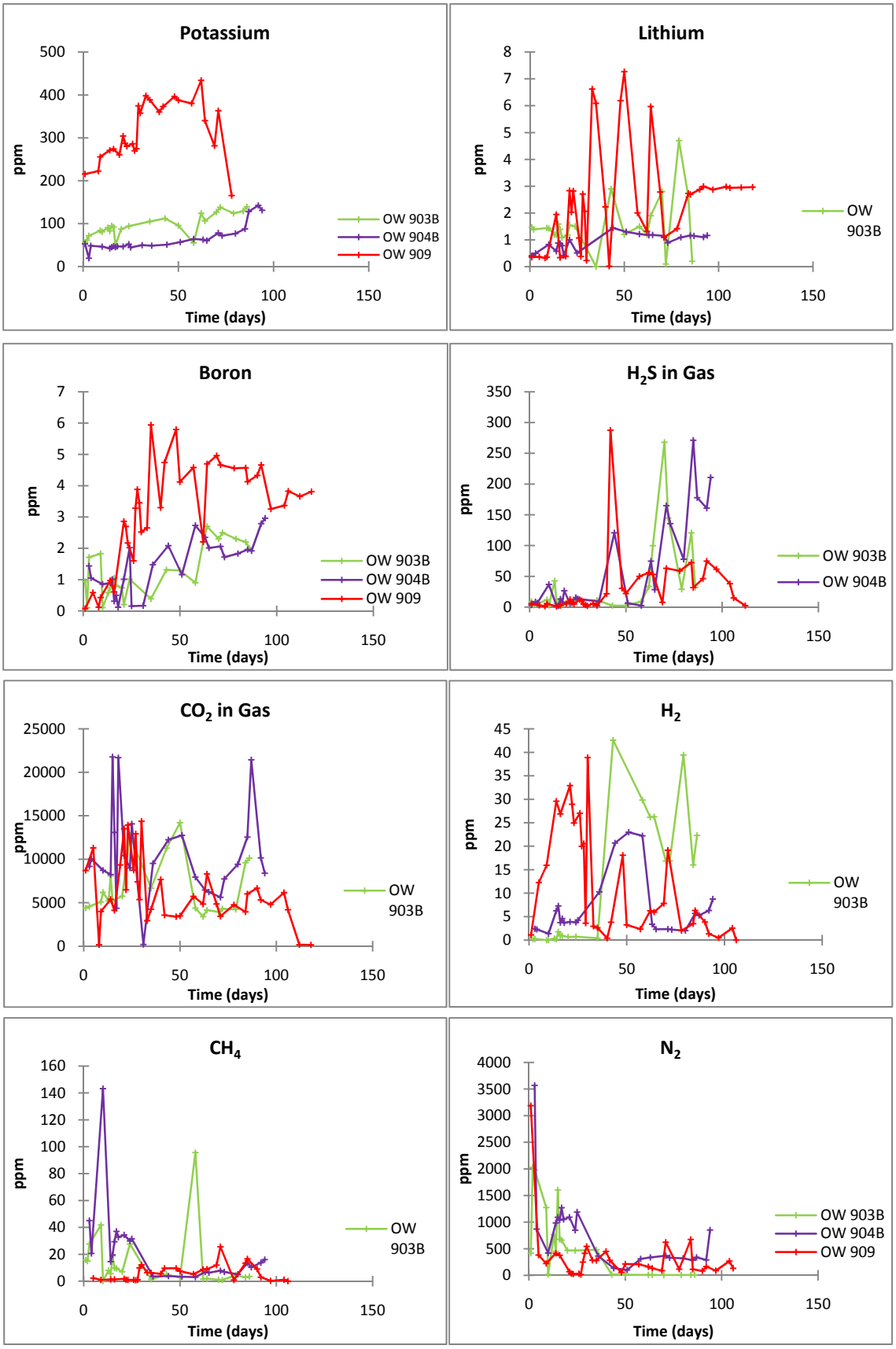

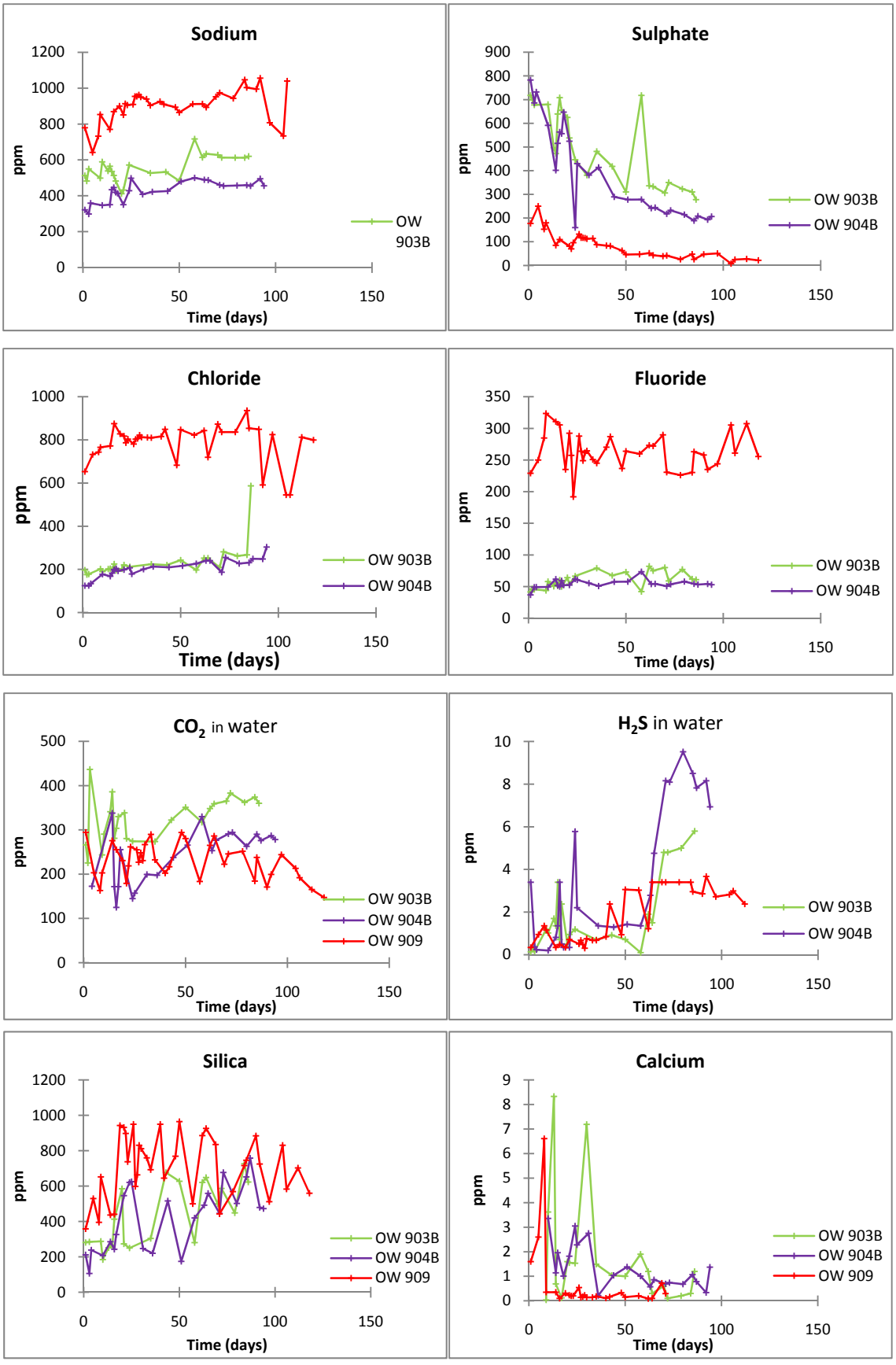
Sodium
ppm
Time (days)
OW 903B
Sulphate
ppm
Time (days)
OW 903B
OW 904B
Chloride
ppm
Time (days)
OW 903B
OW 904B
Fluoride
ppm
Time (days)
OW 903B
OW 904B
CO2 in water
ppm
Time (days)
OW 903B
OW 904B
OW 909
H2S in water
ppm
Time (days)
OW 903B
OW 904B
Silica
ppm
Time (days)
OW 903B
OW 904B
OW 909
Calcium
ppm
Time (days)
OW 903B
OW 904B
OW 909

**APPENDIX III: Deep fluid chloride concentration in the Olkaria Domes wells correlated with other elements**